



<https://theses.gla.ac.uk/>

Theses Digitisation:

<https://www.gla.ac.uk/myglasgow/research/enlighten/theses/digitisation/>

This is a digitised version of the original print thesis.

Copyright and moral rights for this work are retained by the author

A copy can be downloaded for personal non-commercial research or study,
without prior permission or charge

This work cannot be reproduced or quoted extensively from without first
obtaining permission in writing from the author

The content must not be changed in any way or sold commercially in any
format or medium without the formal permission of the author

When referring to this work, full bibliographic details including the author,
title, awarding institution and date of the thesis must be given

Enlighten: Theses

<https://theses.gla.ac.uk/>
research-enlighten@glasgow.ac.uk

A STUDY OF THE SMALL INTESTINE AS A LIMITING
NORMAL TISSUE IN RADIOTHERAPY

by

Roy Hamlet, B.Sc., M.I. Biol.

A thesis presented to the University of Glasgow
for
The Degree of Doctor of Philosophy

September, 1980

Radiobiology Research Group
Glasgow Institute of Radiotherapeutics and Oncology,
Belvidere Hospital,
Glasgow G31 4PG.

ProQuest Number: 10778149

All rights reserved

INFORMATION TO ALL USERS

The quality of this reproduction is dependent upon the quality of the copy submitted.

In the unlikely event that the author did not send a complete manuscript and there are missing pages, these will be noted. Also, if material had to be removed, a note will indicate the deletion.



ProQuest 10778149

Published by ProQuest LLC (2018). Copyright of the Dissertation is held by the Author.

All rights reserved.

This work is protected against unauthorized copying under Title 17, United States Code
Microform Edition © ProQuest LLC.

ProQuest LLC.
789 East Eisenhower Parkway
P.O. Box 1346
Ann Arbor, MI 48106 – 1346

Thesis
6267
Copy 1.

CONTENTS

	Page
CONTENTS	i
ILLUSTRATIONS	v
TABLES	viii
ACKNOWLEDGEMENTS	ix
SUMMARY	xi
CHAPTER 1	INTRODUCTION AND REVIEW OF THE FIELD OF INVESTIGATION
1.1	Introduction 1
1.2	Subjects of Investigation 4
1.3	Reasons for Choice of Assay System for Investigation of CRE Model 6
1.4	Literature Review 7
1.4.1	The Structure of the Bowel and Cell Renewal System of the Intestinal Epithelium 7
1.4.2	Assay of Intestinal Radiation Damage by the Measurement of Crypt Regeneration 10
1.4.3	Intestinal Surface Morphology as an Indicator of Experimental Radiation Injury 13
1.4.4	The Cumulative Radiation Effect (CRE) 18
CHAPTER 2	MATERIALS AND METHODS
2.1	Animals 22
2.2	Irradiation Procedures and Dosimetry 22
2.3	Tissue Preparation and Microscopy 26
CHAPTER 3	CRYPT SURVIVAL AND SURFACE MORPHOLOGY AFTER

		Page
	SINGLE WHOLE BODY DOSES OF NEUTRON AND GAMMA IRRADIATION	
3.1	Introduction	28
3.2	The Experiments	30
3.3	Crypt Regeneration after Irradiation	31
3.4	Scanning Electron Microscopy. Controls	33
3.5	Distension	33
3.6	'Shoulder' Doses	36
3.7	Higher Doses	38
3.8	Low Doses	39
3.9	Discussion	43
CHAPTER 4	CRYPT SURVIVAL AND SURFACE MORPHOLOGY OF THE GUT AFTER FRACTIONATED DOSES OF X AND γ IRRADIATION	
4.1	Introduction	45
4.2	The Experiments	45
4.3	Regenerating Crypts	47
4.4	Presentation of Crypt Data	49
4.5	Animal Condition and Postmortem Observations	49
4.6	Scanning Electron Microscopy	51
4.7	Damage Assessment Using SEM	52
4.8	Controls	53
4.9	SEM Damage Assessment in the Three Schedules	55
4.10	Discussion of Results	60
CHAPTER 5	A BIOLOGICAL INVESTIGATION OF THE	

	Page
ALTERNATING FRACTIONATION FORMULA OF THE CRE MODEL	
5.1	Introduction 72
5.2	The Experiments 73
5.3	The Standard Schedule 73
5.4	Results 76
5.5	Discussion 79
CHAPTER 6 A BIOLOGICAL INVESTIGATION OF THE GAP FORMULA OF THE CRE MODEL	
6.1	Introduction 82
6.2	The Experiments 84
6.3	Gap Experiments 86
6.4	Comparison of the Results with the Predictions of the CRE Gap Formula 88
6.5	Discussion and Conclusions 93
CHAPTER 7 SUMMARY OF CONCLUSIONS AND DISCUSSION OF SOME POSSIBLE FUTURE DEVELOPMENTS	
7.1	Introduction 97
7.2	Surface Morphology after Single Doses of Neutron Irradiation 97
7.3	Surface Morphology after Fractionated Doses of X and Gamma Irradiation 98
7.4	The Alternating Fractionation Formula of the CRE Model 99
7.5	The Gap Formula of the CRE Model 100

	Page	
7.6	Further Work: Experiments Commenced	102
7.7	Some Possible Future Developments	103
APPENDIX I		105
APPENDIX II		108
REFERENCES		114

ILLUSTRATIONS

		Page
Chapter 3		
Figure 3.1	Dose-response curves of crypt survival after single doses of D-T neutron and ⁶⁰ Cobalt gamma irradiation.	32
Figure 3.2	Specimen from control animal. SEM of normal mouse jejunum after standard distension (x100).	34
Figure 3.3	SEM of normal mouse jejunum which has been over distended (x100).	34
Figure 3.4	SEM of underdistended normal mouse jejunum (x200).	35
Figure 3.5	SEM of mouse jejunum after 1000 rads of ⁶⁰ Cobalt gamma irradiation (x100).	37
Figure 3.6	SEM of mouse jejunum after 500 rads of D-T neutron irradiation (x100).	37
Figure 3.7	SEM of mouse jejunum after 1600 rads ⁶⁰ Cobalt gamma irradiation (x100).	40
Figure 3.8	SEM of mouse jejunum after 800 rads of D-T neutron irradiation (x200).	40
Figure 3.9	SEM of mouse jejunum after 300 rads of ⁶⁰ Cobalt gamma irradiation (x200)	42
Figure 3.10	SEM of mouse jejunum after 170 rads of D-T neutron irradiation (x200).	42

	Page
Chapter 4	
Figure 4.1	48
Crypt survival curves for schedules A, B and C and single doses of ⁶⁰ Cobalt gamma irradiation.	
Figure 4.2	54
SEM of control specimen. A good quality control showing well defined finger like villi (x100).	
Figure 4.3	54
SEM of control specimen chosen for its relatively poor quality (x100).	
Figure 4.4	56
SEM from Schedule A, of a specimen which received a total dose of 3000 rads (x100).	
Figure 4.5	56
SEM from Schedule B, of a specimen which received a total dose of 2250 rads (x100).	
Figure 4.6	59
SEM from Schedule C, of a specimen which received a total dose of 4250 rads (x100).	
Figure 4.7	59
SEM from Schedule C. Total dose 3750 rads showing morphology similar to coeliac disease (x200).	
Figure 4.8A	62
Crypt survival for Schedule A.	
Figure 4.8B	63
Histogram of surface damage in Schedule A.	
Figure 4.9A	65
Crypt survival for Schedule B.	
Figure 4.9B	66
Histogram of surface damage in Schedule B.	
Figure 4.10A	68
Crypt survival curve for Schedule C.	
Figure 4.10B	69
Histogram of mucosal damage in Schedule C.	

	Page
Chapter 5	
Figure 5.1	78
Crypt survival curves for the standard and alternating fractionation schedules.	
Chapter 6	
Figure 6.1	85
Crypt survival curve for the standard schedule.	
Figure 6.2	89
Graphic representation of the results of the assay doses of the gap schedules.	
Figure 6.3	91
Theoretical total dose required to achieve the same end point, plotted as a function of the position of the gap.	
Figure 6.4	92
Experimental results presented in same format as figure 6.3.	
Figure 6.5	95
Hypothetical representation of how regeneration potential varies with increasing total dose.	
Appendix I	
Figure A1	106
Diagram of shielding unit.	
Appendix II	
Figure A2	109
Results of split dose experiments.	
Figure A3	112
Photograph of mouse showing classic post-irradiation pigment loss in irradiated area.	

TABLES

	Page
Table I Treatment strategy	75
Table II Results of the schedules	77
Table III Results of gap experiments	87

ACKNOWLEDGEMENTS

I would like to thank Dr. J. Kirk of the Radiobiology Research Group, Belvidere Hospital, Glasgow, Professor A.H.W. Nias, now at the Richard Dimbleby Department of Cancer Research, St. Thomas' Hospital, London and Dr. K.E. Carr of the Department of Anatomy, Glasgow University, for their invaluable help and advice during the course of this work.

In particular I would like to acknowledge the collaboration with Dr. K.E. Carr, Professor A.H.W. Nias and Dr. P.G. Toner (of the Department of Pathology, Glasgow Royal Infirmary) in the scanning electron microscope studies detailed in Chapters 3 and 4 and with Dr. J. Kirk and Dr. A.M. Perry (of the Department of Clinical Physics and Bioengineering, Glasgow) in the work on the CRE model described in Chapters 5 and 6.

I would like to thank Mrs. Margaret O'Donnell of the Radiobiology Research Group for assistance with the animal irradiations and Mr. G.A. Gillespie and Mrs. Christine Watt of the Department of Anatomy for their help with the histology and scanning electron microscopy tissue preparations.

I am indebted to Drs. R.C. Lawson and R. Strang of the Department of Clinical Physics and Bioengineering for assistance with the neutron and Cobalt 60 dosimetry and Dr. A.M. Perry for his help with the X-ray dosimetry and the statistics in Chapter 6, and for their helpful discussions.

My thanks are due to Professor R.J. Scothorne for the use of the Scanning Electron Microscope in the Department of Anatomy, Glasgow University, and I would also like to

thank Professor J.N.A. Lenihan, Director of the Department of Clinical Physics and Bioengineering and Dr. G. Flatman, Director of the Glasgow Institute of Radiotherapeutics and Oncology for their continued support.

I'm grateful thanks to Mrs. Grace Logan for typing this thesis.

This research work was supported by an M.R.C. grant awarded to the Glasgow Institute of Radiotherapeutics and Oncology.

SUMMARY

In clinical radiotherapy the dose to a tumour is limited, in any particular instance, to the dose which can be tolerated by the surrounding normal tissues. The experimental work described in this thesis deals with an investigation of one of these limiting normal tissues, the gut. The animal system chosen was also used to investigate some of the predictions of one of the mathematical models devised to estimate normal tissue tolerance in clinical situations. This was the CRE (Cumulative Radiation Effect) model.

This thesis consists of seven chapters; the First Chapter contains a brief introduction, a description of the proposed research and a review of the background literature. The literature review is not totally comprehensive but was chosen to introduce data and information about the animal system used in the research, the experimental methods which were employed and the mathematical model investigated.

The Second Chapter, entitled Materials and Methods, describes the experimental animals and the conditions in which they were housed; the irradiation and dosimetry procedures and the methods used for the preparation and examination of the tissue specimens removed from the irradiated and control animals.

Chapter Three describes intestinal crypt survival and scanning electron microscopy of the mucosa of the small intestine after single whole body doses of neutron or gamma irradiation. The results obtained demonstrate that scanning electron microscopy of the surface mucosa of the intestine, although difficult to quantitate, is a much more sensitive indicator of

intestinal damage at low dose levels than the more standard methods involving the enumeration of surviving crypts of Lieberkuhn in a section of intestine. Being a direct method of observation it is likely to be more accurate than the usual extrapolation from the exponential fall of crypt numbers after high doses of irradiation (ie. greater than 500 rads neutrons or 900 rads gamma rays). The results also demonstrate that the morphology of the *Jejunal* mucosa follows a different pattern following neutron irradiation than the pattern seen after gamma irradiation.

Chapter Four contains a description of intestinal crypt survival and surface morphology after fractionated doses of X and gamma irradiation. The results show that there is a lack of correlation between the damage expressed in terms of either crypt survival or mucosal damage in two out of three fractionated schedules. These observations are discussed in terms of their relevance to therapy situations.

The Fifth Chapter describes an investigation of the alternating fractionation formula of the CRE model. It can be seen that of the two major predictions of the formula only one is confirmed by the experimental results. There is a discussion of the possible reasons underlying these differences and similarities and an assessment of the formula in general use.

Chapter Six contains a description of an investigation of the CRE formula which deals with the allowances that must be made when gaps occur in fractionated irradiation schedules. There is a comparison of the results with the predictions of the formula and a discussion of the factors which must be taken into

account to try and overcome some of the shortcomings of the model.

Chapter Seven is a summary of the conclusions drawn from the experimental research. It also contains a section dealing with possible further work suggested by the experimental results. The Appendices, which follow the conclusions chapter, contain descriptions of one of the irradiation facilities and some of the more important ancillary experiments.

CHAPTER 1

INTRODUCTION AND REVIEW OF THE FIELD OF INVESTIGATION

1.1. Introduction

The 20th century has witnessed the evolution of the use of ionising radiation as a therapeutic agent. Some early success with radiation treatment led to a wave of optimism which was to be suppressed when a number of serious side effects were discovered. Thereafter improvement was a slow, painstaking and often hazardous process, which relied in the earlier years on the intuition, skill and observation of clinicians. However, improvements in the physical and technological aspects of radiotherapy, plus an increasing understanding of the biological effects have increased the variety of malignant conditions for which radiotherapy offers a good prognosis. In perhaps fifty per cent of cases it is now the treatment of choice. In the last thirty five years particularly, information relevant to the practice of clinical radiotherapy has been steadily augmented by advances in many fields and some relevant examples will be discussed later.

It must be remembered, however, that one of the basic problems facing the clinician is that the dose that can be administered to any tumour is limited by the amount of radiation damage that can be tolerated by the normal tissues in the treated volume. This fact was realised very early on and is a contributory and important reason why treatments are administered as fractionated schedules, which allow intervals between the radiation doses for differential repair and repopulation of the normal tissues

whilst giving a high total dose to the tumour. These intervals also allow time for repopulation of the neoplastic tissue and hence the development of clinical schedules has progressed mainly on empirical lines derived from clinical observation. Thus it is necessary for the experimentalist to remember the importance of assessing and investigating the effects of radiation in normal tissues.

Help has been forthcoming from many research areas as mentioned earlier, and some of the discoveries have been implemented in clinical practice in recent years; it may be helpful to give examples of some of the more recent advances. It has been recognised that the presence of oxygen in tissues enhances the effect of electro-magnetic radiations such as X and gamma rays which are described as having a low LET or linear energy transfer. The realisation that tumours commonly contained a proportion of hypoxic cells has led to the use of hyperbaric oxygen and high LET irradiation sources such as neutron generators in an attempt to kill more tumour cells compared to the number of normal cells; in fact, to try and increase the therapeutic ratio. Similarly the field of biochemistry has produced ELECTROAFFINIC drugs and some of these are being used in clinical trials at present to assess their ability to modify the radiosensitivity of tumour cells.

Many of the advances in biology have been important to the understanding of the response of individual cells,

cell populations and tissues to radiation. The use of in vitro and in vivo techniques has led to a better understanding of the nature of the cell cycle, cell population kinetics and the mechanisms of repair and repopulation. In the field of mathematics models have been produced to try and explain these observations; many of these models are of such complexity that computers have been used to try and correlate the many factors involved, with the hope that they might contribute to the production of 'optimal' treatment schedules. These schedules will try and make use of any differences in the repopulation kinetics of normal or neoplastic tissues to the detriment of the latter.

These few examples are given purely to illustrate how the results of research effects the understanding of the basic problems underlying radiotherapy treatment and how in some cases they have led to the innovation of new methods of treatment for use by the clinicians. Many of the research programmes have been aimed at ways to increase the numbers of tumour cells which are killed during treatment and undoubtedly much more basic research into the biology of tumour systems and the development of new methods of treatment will be carried out. However it is an intrinsic problem in the field of cancer therapy that there is as yet no agent which can differentiate between normal and neoplastic tissue and this fact emphasises the value of continued research into the function and structure of normal tissues.

1.2. Subjects of Investigation

The research work described in this thesis is an investigation of radiation effects on the small intestine or ileum of the mouse. This is a very radiosensitive organ and it is because of this characteristic which severely limits the dose of radiation to any area involving this tissue, that it is sometimes known as one of the 'limiting normal tissues'.

The experiments are divided into two main groups. The first group of experiments involve a comparison of radiation effects as described by scanning electron microscopy of the surface mucosa of the small intestine and radiation effects as assayed by the depletion of the numbers of crypts of Lieberkuhn in the intestine. The second assay system is similar to that developed by Withers and Elkind (1970), which is sometimes known as the microcolony assay technique and involves the enumeration of the surviving numbers of crypts in a circumferential section of intestine as a measure of radiation damage. Both methods are used to compare the effects of single whole body doses of D-T neutron or ⁶⁰Cobalt gamma irradiation, and fractionated whole or partial body doses of X or gamma rays. The fractionated doses were administered in three separate schedules which were devised to mimic schedules in common use in clinical practice.

As scanning electron microscopy (SEM) is used to observe the 'functional' compartment of the gut it was

hoped that a comparison with a method which assayed damage to the proliferative compartment of the gut might give an insight into the various patterns of radiation injury in the whole organ.

The second group of experiments are concerned with the investigation of some of the predictions of the CRE (cumulative radiation effect) model. Various formulae have been derived from observations of clinical data to assess radiation damage to normal tissue (usually skin or normal connective tissue, another of the limiting normal tissues). The formulae are used as an aid to planning clinical treatments and some are in use in many radiotherapy centres. Perhaps the ones in most common use at present are the NSD (Ellis, 1968) the TDF (Orton and Ellis, 1973) and the CRE (Kirk et al., 1971).

The experiments used the Withers microcolony technique purely as a measure of biological damage. The effects of alternating large and small sized fractions were investigated and the results compared with the predictions of the alternating fractionation formula of the CRE model. A second and larger set of experiments investigates the effects on repopulation when a gap occurs in a treatment schedule and how these effects are modified by the position of the gap in the schedule. The results obtained are compared with the predictions of the gap formula of the CRE model for the same conditions.

1.3. Reasons for Choice of Assay System for Investigation of CRE Model

The CRE model was derived from clinical observations of the effects of radiation on human skin, as is clinically applicable to normal connective tissue. The end point (or amount of damage) is quoted as a CRE value on a CRE scale of damage. Obviously this scale does not apply to the more radiosensitive organ, gut. However the general predictions of the formulae should, if they are to be of any use clinically, be applicable to all normal dividing tissues. In this work gut was chosen as the animal model because it is one tissue in which a direct measure of radiation damage can be obtained by counting the numbers of regenerating crypts present in a section of tissue. It is therefore not necessary to devise a scale of measurement of damage, thus overcoming the main criticism of work with irradiated skin, that the method of assessment of damage can at best only be very subjective.

1.4. Literature Review

The experimental work in this thesis deals with an investigation of an animal model of a 'limiting normal tissue' as the term is used in the context of clinical radiotherapy. This animal model, the mouse ileum, was also used to test some of the predictions of a mathematical model devised to assess the biological effect of radiation on normal connective tissue in clinical situations, the CRE (Cumulative Radiation Effect). This literature review is not intended to be totally inclusive but is chosen to introduce information about the animal system, the experimental methods employed and the mathematical model investigated.

1.4.1 The Structure of the Bowel and the Cell Renewal System of the Intestinal Epithelium

The digestive tract consists of the mouth, pharynx, oesophagus, stomach, small intestine, large intestine and rectum. However, subsequent discussion is limited to the small intestine as its response to radiation injury is the subject of this investigation.

In the small intestine three regions can be distinguished, the duodenum, jejunum and ileum. Their structures, although showing some differences, are basically the same in principal and so one description applies to them all. In cross section the mucosa is seen to contain innumerable villi lined by a columnar epithelium consisting of mucus and 'chief' cells (Leblond

and Walker, 1956). The crypts of Lieberkuhn which contain the generative cells for epithelial replacement are found in the mucosa at the bases of the villi. Cell renewal occurs in the mitotic areas in the crypts, from here newly formed cells migrate out of the crypts and move from the base of the villi to the top, known as the extrusion zone. The predominate cell in this renewal system is the columnar or 'chief' cell. Scattered among these are goblet cells. At the bottom of the crypts are the cells of Paneth and the argentaffine cells whose precise role is as yet to be fully established.

From the view point of cell kinetics, the epithelial cell renewal system of the intestine can be considered as consisting of four pools. As in any cell renewal system there must be a stem-cell pool which is self-sustaining. In the intestine the stem cell has not been morphologically identified, but the area of cell proliferation is known to be the walls of the crypts. It is therefore not possible to distinguish morphologically a stem cell from the proliferating pool and the two must be considered together. However, an amplifying or proliferating pool is most likely present. The cells move from the crypts, lose their proliferating capacity, and move into a maturation pool probably located at the neck of the crypts and base of the villi. Early electron microscope studies of the maturation pool demonstrated the occurrence of cytological changes. Quastler and Hampton (1962)

described these as a cytoplasmic transition from the vesicular proliferative cell to the tubular mature cell. Once the cells are at the base of the villi, they move up the villus surface until they are eventually 'shed' at the villus tip or extrusion zone.

The most accurate estimate of time parameters of cell renewal in the intestinal epithelium has been derived from studies using tritiated thymidine (e.g. Quastler and Sherman, 1959; Sherman and Quastler, 1960; Fry et al., 1961; Leshner et al., 1961; Lipkin and Quastler, 1962). However estimates have also been made from mitotic indices (Leblond and Stevens, 1948, Bertalanffy et al., 1962). Relative turnover times for various regions of the gastrointestinal tract have been calculated by many experimental workers and from comparative values it is evident that the small intestine has the most rapid cell renewal. In the mouse the cell doubling time in the jejunum is approximately 12 hours.

The parameters of villus transit time have been estimated by the use of tritiated thymidine, as the time elapsed from the first appearance of labelled cells at the base of the villi until the first labelled cells are shed from the villus tip. The villus transit time in man is about three to four days, two to three days in the rat and one to two days in the mouse. However, since these parameters were obtained from the movement of the fastest cells these times are minimum estimates, and the values must be considered as guides only as the times

vary from strain to strain in the same species and also with age (Leshner et al., 1961, Fry et al., 1962).

Furthermore the studies in man were performed in patients with malignant disease, which may have influenced the time parameters (Lipkin et al., 1963).

Estimates of transit time through the maturing pool have been made and most estimates are within the limits of 2 to 4 hours. As the number of generations between stem-cell division and the last proliferative division is not known the transit time in the proliferative pool is not known.

This brief description of the structure and cell kinetics of the normal intestinal mucosa is given to serve as a basis for the discussion of the effects of radiation on the intestine in the following sections.

1.4.2 Assay of Intestinal Radiation Damage by the Measurement of Crypt Regeneration

A technique for measuring survival rates of crypt cells following irradiation was described by Withers and Elkind (1970). Mice were killed three and a half days after an acute dose of irradiation, a section of small intestine removed, fixed and examined histologically. A control (unirradiated) value of 160 crypts per circumference of intestine in mouse jejunum was observed. After large doses of radiation a proportion of the crypts were completely depopulated of clonogenic cells and thus there were fewer regenerating crypts counted three and a

half days after irradiation than in the control animals. The fall in crypt numbers with increasing dose can be plotted to give a crypt survival curve. This is a brief description of what has come to be known as the crypt micro-colony assay system, and it was this system that was chosen as the quantitative biological assay system for the experiments described in the later chapters.

In order to define a crypt cell survival curve Withers and Elkind assumed that crypt cells survived independent of one another, that one surviving clonogenic cell was sufficient for the regeneration of a crypt and that the number of surviving cells in a crypt were randomly distributed. Using Poisson statistics the average survival per crypt could be calculated and hence the cell survival per circumference of intestine. Cell survival curves could then be plotted using the crypt survival data.

Withers, Brenman and Elkind (1970) used this technique to investigate the effects of X-rays and neutrons on crypt cells. This allowed them to study the radiobiological effectiveness (RBE) of neutrons compared with X-rays at a cellular survival level. Their figures demonstrated that RBE values for cell survival were similar to published RBE values of 1.4 for LD_{50/5} survival (ie intestinal death following whole body irradiation). Briefly, this suggested that a dose of neutrons is more effective in cell killing by a factor of approximately 1.4 than the same dose of X-rays.

Hornsey (1970) used the micro-colony technique to study variations in survival after electron irradiation at different dose rates and reported that at lower dose-rates a larger dose is required to give the same level of survival.

The same technique was used by Withers et al. (1975) to investigate the effects of fractionated gamma irradiation and fractionated gamma and fractionated neutron irradiation (Withers et al., 1974), where it was reported that there appeared to be little sparing of jejunal mucosa as a result of repair of sub-lethal damage during intervals between neutron dose fractions but considerable repair between fractions of gamma ray doses.

Hendry et al. (1975) used the technique to investigate daily neutron fractionation regimes and reported RBE values of 3.3 for 10 fractions and 3.6 for 15 fractions. A similar technique was used to investigate the survival characteristics of the proliferative cells of the gastric mucosa (Chen and Withers, 1972) and discussed the large sub-lethal repair capacity observed with relevance to radiotherapy treatments involving the stomach.

A different method of measuring crypt survival has also been used extensively to study intestinal irradiation damage. This method (Hagemann et al., 1970) involves the labelling of crypt cells with tritiated thymidine prior to dissection using the technique of

Wimber et al. (1960). By determining the activity of aliquots of labelled crypts it is possible to plot a graph of crypt survival against increasing dosage of radiation. This technique employs a correction factor for weight changes following irradiation.

This technique has been used extensively to determine the effects of single doses (Hagemann et al., 1971) and fractionated doses (Hagemann et al., 1971) of X-rays on crypt survival; the effects of oxygen on crypt survival in irradiated mice (Sigdestad et al., 1973), the effects of different types of irradiation (gamma, X-rays and neutrons) on crypt survival (Sigdestad et al., 1972) and the degree of intestinal cell proliferation during fractionated irradiation (Hagemann, 1976).

These and many other studies have produced valuable information on the response of the proliferative compartment of the small intestine to many types of irradiation and under various conditions of oxygenation and hypoxia.

1.4.3 Intestinal Surface Morphology as an Indicator of Experimental Radiation Injury

Apart from the maintenance of the proliferative capacity of a tissue, the clinical radiotherapist is also concerned with the maintenance of the functional ability of that tissue. In the gut the functional compartment (the villi) is dependent not only on the ability of the cells in the crypts to proliferate but also on their

ability to leave the proliferative pool and mature as functioning cells; loss of gut function, even for a very short time, after irradiation can have drastic consequences for the patient. The dissecting microscope was first used to examine the mucosal surface of the small intestine (Rubin et al., 1960) and in 1961 Holmes, Hourihane and Booth (1961 a and b) demonstrated its diagnostic use when they described the mucosal changes in coeliac disease and tropical sprue. Studies of this kind brought more understanding of mucosal structure but advances were limited by the low resolving power of the dissecting microscope, until Marsh, Swift and Williams (1968) introduced the scanning electron microscope as a method of examining mucosal structure in greater detail, although the first preliminary studies (and perhaps the first use of SEM for the study of soft tissue) were done by Jaques, Coalson and Zervins in 1964 (Jaques et al., 1965).

The following is a brief description of how the scanning electron microscope works. (Taken from Marsh Swift, 1969). A beam of high energy electrons accelerated from a heated tungsten filament is focused into a narrow probe the size (diameter) of which can be varied by means of two electromagnetic lens. A third electromagnetic lens focuses the electron probe onto the specimen and scanning coils in this lens move the probe over the surface of the specimen. Secondary electrons emitted by the specimen are attracted towards a

positively charged Faraday cage, pass through a wire gauge at the cage surface and are accelerated by an applied potential difference. The electrons strike an aluminium-coated plastic scintillator and the light generated passes down a light guide into a photomultiplier which amplifies the signal. This signal is used to modulate a light spot scanning the screen of a television display tube, which is in synchrony with the electron probe. The images produced are related to the surface topography of the specimen under examination. Changes in magnification are made by varying the area of the specimen scanned by the probe. Because the primary beam diverges over a small angle the depth of focus is very large, this of course is a major advantage of the SEM as it produces a three-dimensional perspective to the micrographs obtained.

The scanning electron microscope was used by Larsh and Swift (1969) to examine specimens of jejunal mucosa obtained from subjects undergoing operative treatment where disease of the small intestine was excluded in all the patients. They described finger shaped villi with broad bases tapering to blunt points and remarked on the variation in villous shape, some being circular in cross section whilst others were flattened and tongue or leaf shaped. They described the ridged and corrugated surface of the villi and demonstrated the great depth of focus of the scanning electron microscope by describing epithelial cell boundaries, goblet cell orifices, crypt mouths and

even occasional red blood cells on the villous surface. They also demonstrated that at higher magnifications (x 20,000) the microvilli could be distinguished as discrete structures.

In the same year Toner and Carr (1969) published a paper describing SEM studies of human small intestine specimens and specimens from rats. They also reported the leaf, tongue and finger shaped villi in human specimens and noted that ridges of moderate length were not uncommon. They showed that the leaf shape villous pattern was the normal pattern for the rat and their failure to resolve individual microvilli demonstrated the importance of tissue preparation techniques in obtaining high definition micrographs. Since these publications the scanning electron microscope has been used in a large number of investigations of normal and diseased small intestine in man and several other species and also the effects of gamma irradiation in the mouse intestine (Carr and Toner, 1972) and rat intestine (Anderson and Withers, 1973).

Carr and Toner examined the intestinal surface changes produced in mice by large doses (1500 to 2500 rads) of gamma rays and compared them with some features of human coeliac disease. They noted that 48 hours after irradiation the villi began to lose their normal stability and appeared to droop and clump together. 70 hours after exposure the villi were shorter, more tapered and had developed a conical shape. Some 90 to 100 hours

post-irradiation the mucosal surface showed gross abnormalities. In some cases the villi still existed as discrete stunted projections, but in other cases as only small irregular excrescences which had lost the orderly grooves of the controls and appeared to have warty blebs or projections and to have lost all surface organisation. The authors noted that these appearances were not characteristic of that seen with coeliac disease despite the absence of villi.

Anderson and Withers used the scanning electron microscope to examine the intestine of rats irradiated with 1000 rads ⁶⁰Cobalt gamma rays. The animals were killed at 24 hour intervals after irradiation. 24 to 48 hours after irradiation the morphology of the intestine appeared similar to that of the controls. Mucosal deterioration was at its worst on days three and four, the villi were shorter and sometimes fused. The mucosal floor was no longer smooth and the crypt orifices difficult to distinguish. By the fifth and sixth day post-irradiation morphological repair was evident, and animals examined on days seven to twelve displayed a morphologically normal mucosa.

Following on from the work described in these last two sections the investigations described later in chapters three and four are an attempt to examine the effects of single and fractionated doses of X, gamma and neutron irradiation on the small intestine, from the end points of micro-colony assay and scanning electron

microscopy.

1.4.4 The Cumulative Radiation Effect (CRE)

One of the problems confronting the clinical radiotherapist is the rationalisation of the biological effects of fractionated radiation regimes in the treatment of neoplastic disease. These regimes vary from one treatment centre to another and in order to compare the results from different regimes it is necessary to have some criterion against which they can all be assessed. Ideally, such a rationalisation criterion would provide a method of measurement of the radiation damage to both the normal and neoplastic tissues for any particular treatment regime, thus allowing the comparison of the biological effects of different regimes and also a selection of the most beneficial form of treatment for any particular tumour type.

A significant step towards this ideal was made by Ellis and his colleagues (Ellis, 1967; Ellis 1968; Ellis, 1969; and Winston, Ellis and Hall, 1969). They demonstrated that a single figure representing normal connective tissue tolerance to radiation could be used to designate any course of radiation treatment which reaches tissue tolerance. In practice tolerance is the upper limit of any radiation schedule, and might be defined in terms of the normal tissue as the maximum amount of biological damage that can be sustained by a

tissue from which it can repair without sustaining any permanent disability.

Ellis termed this figure the NSD (nominal standard dose) and showed that it could be expressed mathematically as:-

$$\text{NSD} = (\text{Total Dose}) \cdot N^{-0.24} \cdot T^{-0.11}.$$

where the total dose is given in rad, N is the number of fractions in a treatment and T is the total treatment time. This equation, based on iso-effect curves for different fractionation schedules for squamous cell carcinoma, skin erythema and normal tissue tolerance (Cohen, 1960), applies only to normal tissue at the limit of tolerance as stated previously.

The cumulative radiation effect (CRE) is a generalised form of this NSD empirical function and can be considered as a sum of the effects of fractions or groups of fractions and also takes into account the effects of previous fractions. In other words the CRE is a series of numbers describing a scale of damage, the top of this scale being the same as the NSD. The advantage of this is that schedules can be assessed at sub-tolerance levels of damage. Cumulative radiation effect (CRE) was termed by Kirk, Gray and Watson (1971) and was derived in order to extend the approach of Ellis to the rationalisation of radiotherapy treatment regimes at sub-tolerant levels of damage. The authors have now applied the CRE to a variety of conditions of radiation

treatment in a series of papers. Fractionated Treatment regimes were considered in the above mentioned reference, Continuous Radiation therapy in Kirk, Gray and Watson (1972 and 1973), and Time Gaps in Treatment regimes in Kirk, Gray and Watson (1975).

Although the CRE was derived from a consideration of clinical and experimental data the authors themselves state that limitations are imposed on the CRE by its empirical nature and that any improvement in the CRE concept requires a greater knowledge and understanding of the effects of radiation on normal and tumour tissue in vivo. It is not the purpose of this investigation to analyse the CRE in detail but it was hoped that by testing some of its predictions in an animal system more insight might be gained into how the concept might be made more applicable to the clinical situation. To this end two of the more important predictions of the CRE were chosen for investigation.

In Kirk et al. (1971) it is stated that if a particular regime achieves a certain CRE, its individual fractions may be given in any order whatsoever, without altering the CRE attained. This particular statement is investigated and the results are reported and discussed in chapter five. In Kirk et al. (1975) there is a discussion of how the position of a gap in treatment will effect the amount of additional dose that would be required to achieve the same level of CRE that would be attained by an uninterrupted schedule. These predictions

were investigated and in chapter six the results that were obtained are reported and are discussed in relation to their bearing on the predictions of the CRE model quoted above.

CHAPTER 2

MATERIAL AND METHODS

2.1. Animals

Adult male and female C_3H/He mg mice (supplied by Bantin and Kingman Ltd., Hull) of 10 to 15 weeks of age were used in the experiments. They were housed in plastic cages (12 per cage) in air conditioned rooms, with constant temperature ($21^{\circ}C$) and relative humidity (55%) and maintained in light and dark periods each of 12 hours in duration. (i.e. light:- 7 a.m. to 7 p.m.; dark 7 p.m. to 7 a.m. GMT.)

The animals were provided with formula 41 mouse diet (produced by Angus Milling Company, Perth and supplied by William Shearer and Company, Glasgow) and acidified water (maintained at pH 3.0 with dilute hydrochloric acid) ad libitum, both before and after irradiation. The cages were changed twice weekly and the water daily.

2.2. Irradiation Procedures and Dosimetry

(a) ^{60}Co Cobalt gamma irradiation

The ^{60}Co Cobalt gamma ray exposures were to the whole body and carried out on an Orbitron therapy unit. A perspex jig containing four animals was positioned in the broadest field such that the centre line of each mouse was 40 cm from the source; The animals were irradiated dorso-ventrally. The dose rates to the tissue under these conditions, approximately $180 \text{ rad minute}^{-1}$ over the period of the experiments, were measured using a tissue-equivalent (TE) ionisation chamber designed for the neutron experiments (see below) which was placed at the centre of a perspex mouse phantom located in the jig. The TE chamber had been

had been calibrated against an NPL secondary standard Farmer-Baldwin ionisation chamber under standard conditions.

(b) Neutron irradiation

The neutron irradiations were again to the whole body. During the irradiations, two animals were placed in perspex tubes situated with the long axes parallel to and 8 cm from the plane of the neutron source. The hind 4 cm of the two animals were centralised over the source and during irradiation the tubes were slowly rotated to ensure uniformity of exposure. The source used was a sealed P-tube D-T neutron generator supplied by Elliot Bros. (London) Ltd., which provided primary neutrons of mean energy 14.7 MeV in the direction of the deuterium ion beam incident on the tritium target. Neutron spectrum measurements were available for similar irradiation conditions (Lawson et al., 1972) and the doses received by the animals were estimated to comprise 76% from primary neutrons of 14.7 MeV, 19% from scattered neutrons of mean energy 1.1 MeV and 5% from γ -rays.

The absorbed doses in the neutron field were measured using a small cylindrical ionisation chamber similar in design to that described by Greene (1971). The active length was 16 mm, the outer wall thickness 2.5 mm, the centre electrode diameter 3 mm and the cavity gap 2 mm. The chamber was made from carbon-loaded polythene, which is conducting and approximately tissue equivalent to neutrons. The atomic composition was 10.2% hydrogen and

89.8% carbon by weight. Ethylene gas was flowed through the chamber at constant rate.

The γ -ray sensitivity of the chamber was determined by direct comparison with a Farmer-Baldwin secondary standard ionisation chamber in a ^{60}Co γ -ray field. This factor was used to convert the measured ionisation to the dose which would be absorbed by wet tissue exposed to the radiation field by taking into account neutron kerma values, photon mass energy absorption coefficients, experimental neutron and γ -ray saturation factors for the chamber, assessed W-values, and stopping powers for the charged particle spectra and calibration photons in the gas and walls.

The γ -ray component of the dose was assessed from measurements with LiF TLD/700 chips in teflon and a Geiger-Mueller γ -ray dosimeter. The intrinsic sensitivities of these devices to 14.7 MeV neutrons (0.17 and 0.03 equivalent ^{60}Co rads per neutron tissue rad respectively) were estimated from published data (Wingate et al., 1965; McGinley, 1972; and Goodman, 1972). The uncertainty in the total dose absorbed by tissue from neutrons and γ -rays, deduced from the measurements with the ionisation chamber was $\pm 5\%$. This is similar to that reported by Greene (1971) and by Bewley et al. (1972).

Because the output of the generator could vary, the actual doses given to each pair of animals were controlled by two monitor fission chambers which were placed on the P-tube close to the irradiation jig and regularly calibrated against the TE ionisation chamber placed in a

mouse phantom in the irradiation jig. Dose rates to tissue for the neutron exposures were in the range 5 to 12 rad minute⁻¹.

(c) X-irradiation

Partial body X-irradiations were carried out using a Siemens Stabilipan I unit operating at 250 kV and a filament current of 15 mA. Beam filtration gave a HVL of 1.85 ± 0.05 mm Cu. (The tube of this unit was contained in a specially designed, shielded box which was constructed in the Glasgow Institute of Radiotherapeutics and Oncology. The description of this unit is contained in Appendix 1.)

Mice were restrained in perspex tubes which were positioned so that the abdominal cavity was over a 2.5 cm wide slot cut in a 3 mm thick lead sheet and thus they were irradiated ventro-dorsally. Dose rate measurements were made in a perspex phantom with an ionisation chamber both over the centre of the slot and 1.5 cm from its edge, in the position which the femora were judged to lie. The femoral dose was $< 4\%$ of the intestinal dose.

The suitability of this phantom was checked by comparing this dose rate to measurements made with an ionisation chamber placed in the abdominal cavity of a dead mouse. The difference was $< 3\%$. The dose profile across the slot was determined using LiF thermoluminescent dosimeter. LiF rods were inserted in a perspex block at 0.5 cm intervals, this was positioned over the slot and irradiated. As a check on the relative doses at the

intestines and femora, LiF rods were inserted at these sites in a dead mouse and irradiated. These measurements correlated very well with those made with the ionisation chamber. All dose rate measurements were made using a Farmer-Baldwin dosimeter which had been calibrated against a secondary standard instrument for the energy used. The dose rate obtained 1 cm above the slot was $75 \text{ rad minute}^{-1}$ this being the position of the mouse intestine during irradiation.

2.3. Tissue Preparation and Microscopy

The mice were killed by cervical dislocation three-and-a-half days after the final irradiation dose was administered. Control animals for each experiment were killed at the same time. Two segments of the proximal small intestine, approximately 1.5 cm long, were removed; one for examination under light microscopy and one for examination with scanning electron microscopy. The segments were always taken from the same area, which was approximately 4 cm below the pylorus thus avoiding the duodenum.

The segment for light microscopy was flushed and fixed in 10 per cent formal saline for one to two days then cut into smaller pieces three to four millimetres long. These were embedded in paraffin wax, sectioned transversely (5μ) and stained with haematoxylin and counter-stained with eosin. The number of regenerating crypts per circumference were counted (200 x magnification). In practice the segments

from several mice receiving the same radiation dose were pooled on removal to the fixative.

The segment for electron microscopy was flushed and then gently inflated with fixative, so as to preserve the normal dimensions, the ends were then tied off and the segment immersed in fixative. Two fixatives were used during the course of the experiments, 10 per cent formal saline and 2 per cent phosphate buffered glutaraldehyde at pH 7.4. Following adequate fixation (at least 2 days) the inflated gut was opened longitudinally along the line of the mesentery and washed out with buffer solution. Suitable portions of tissue were post fixed with one per cent Osmium tetroxide in Millonig's buffer for one hour and then washed in water. They were then dehydrated through a series of ethanol solutions of increased concentration up to absolute ethanol. The specimens were pinned out on cork and allowed to dry in air at room temperature.

When dry the rough edges of the samples were trimmed off and these trimmed specimens were then mounted on specimen carriers with conducting adhesive solution and vacuum coated with gold-palladium. The tissues were examined with an S600 scanning electron microscope (Cambridge Scientific Instrument Company) used in the emissive mode at accelerating voltages of from 1.5 kV to 25 kV. Recording was done with 35 mm or 70 mm FP4 film.

CHAPTER 3

CRYPT SURVIVAL AND SURFACE MORPHOLOGY AFTER SINGLE
WHOLE BODY DOSES OF NEUTRON AND GAMMA IRRADIATION

3.1. Introduction

The quantitation of the response of the intestinal epithelium cells to irradiation has been made possible by the development of methods for the assay of intestinal crypt survival (Withers and Elkind, 1970; Withers et al., 1970; Hagemann et al., 1970 and 1971). The disadvantage of such crypt-counting techniques lies in their inability to directly measure damage at lower doses, in the range more commonly used in fractionated radiotherapy. A quantifiable effect is only directly observable after single doses of δ or X-irradiation in the range 1-2 Krad, although a temporary perturbation of the kinetics of the cell population can be observed at lower doses (Lesher, 1967). This effect of irradiation on the cell kinetics of the proliferation compartment is expressed as a failure to maintain epithelium integrity. Since it is not until the number of cells in any particular crypt has been reduced to less than one cell that a reduction in crypt numbers will occur, then stem cell injury caused by lower doses will not be expressed on a regenerating crypt survival curve. It has been shown to be possible to produce a crypt cell survival curve by extrapolation from crypt survival data (Withers et al., 1970), but with the scanning electron microscope it is possible to observe directly the effects of low doses of irradiation on the integrity of the surface mucosa of the intestine (Carr and Toner,

1968; Toner and Carr, 1969). Experiments were devised in an attempt to bring together those qualitative and quantitative approaches and thus build up a more complete picture of the acute intestinal response to irradiation.

3.2 The Experiments

Mice were irradiated with single whole body doses of ^{60}Co Cobalt gamma or 14.7 MeV D-T neutron irradiation over the ranges of 0-2 Krads for gamma and 0-1 Krad for neutron irradiation, gut sections being examined by light and electron microscopy. In addition to the usual controls tests were made of the effects of different degrees of distension by fixative on the gut. Under-inflated and over-inflated segments were compared in both normal and irradiated animals.

RESULTS

3.3. Crypt Regeneration after Irradiation

Figure 3.1 shows dose-response curves following ^{60}Co and D-T neutron irradiation. Both curves have similar final slopes, with D_0 values of 180 and 150 rads respectively. Using this system of representation it is possible to compare the effects of the two different radiations at the same quantitative level of biological damage, expressed as the mean number of surviving crypts per circumference of intestine.

The RBE for D-T neutron compared to γ -radiation falls slightly with increasing dose from 2.1 to 1.8, expressed at several points along the crypt survival co-ordinate. Clearly demonstrated are the large 'shoulders' of the two curves which are attributable to cell multiplicity in the crypt and the accumulation of sublethal damage by the crypt cell. This limits the discrimination of effect of this technique to relatively high dose levels. With γ -irradiation the first significant deviation from the shoulder occurs at around 1,000 rads, whereas in the neutron series the first deviation from the shoulder occurs at doses around 500 rads (an RBE of 2.0).

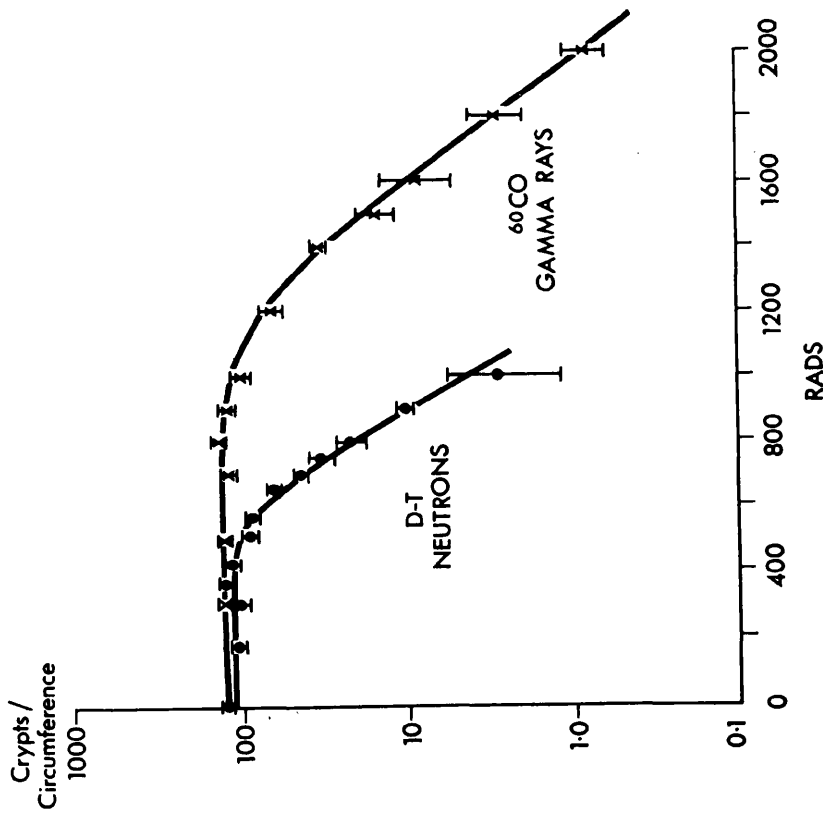


Figure 3.1
 Dose-response curves of mouse jejunal crypt survival after single doses of D-T neutron and ⁶⁰Cobalt gamma irradiation.

Scanning Electron Microscopy

3.4. Controls

Figure 3.2 shows a segment of intestine from an unirradiated control. Although there is a slight variation in the morphology of the villi, over the series as a whole the control animals display structural characteristics in agreement with those described in the literature. The villi are erect, firm and finger like in appearance, they are separate and not clumped or leaning together. The surface creasing is ordered without any very severe indentation.

3.5. Distension

To eliminate possible sources of error, the effects of different degrees of distension of the small intestine by fixative were considered, since a random element was inevitable at this point in the preparation of the specimens. It was found that increasing distension of the normal control intestine (example shown in Figure 3.3) caused increased separation of the villi with some minor variation in their orientation. However, changes in the surface contours of the villi were not seen to be produced by distension.

No bending or twisting of the villi was seen to occur, and the villi were not distorted into conical or leaf patterns. After high doses of neutron or gamma irradiation (i.e. doses which reduced crypt survival to

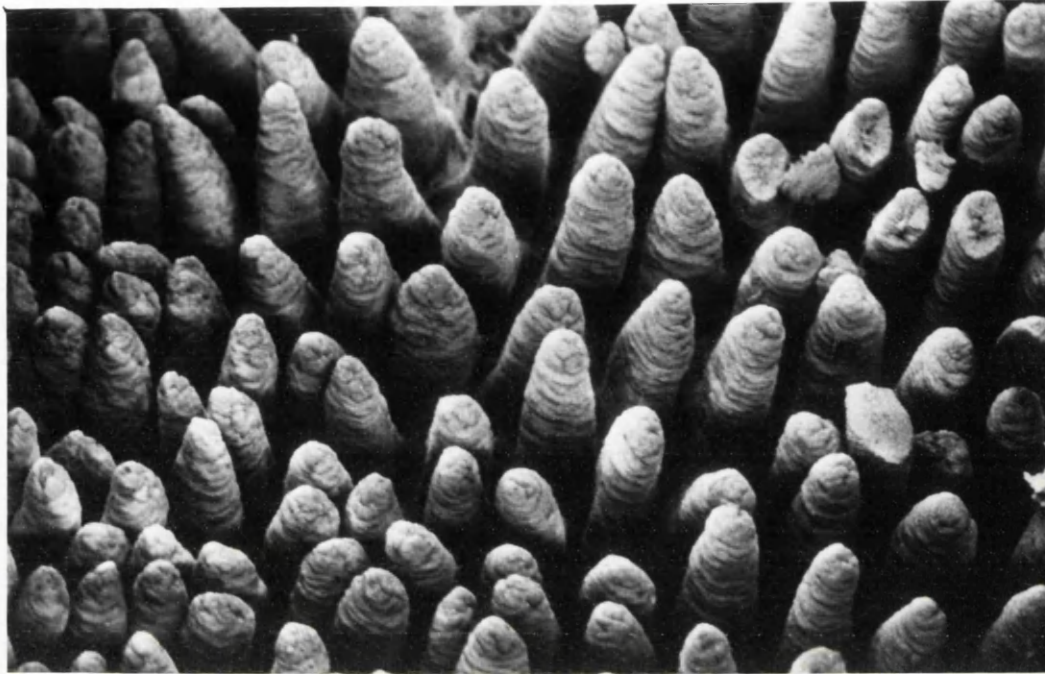


Figure 3.2

Specimen from control animal. Scanning electron micrograph (SEM) of normal mouse *Jejunum* after standard distension (x100).

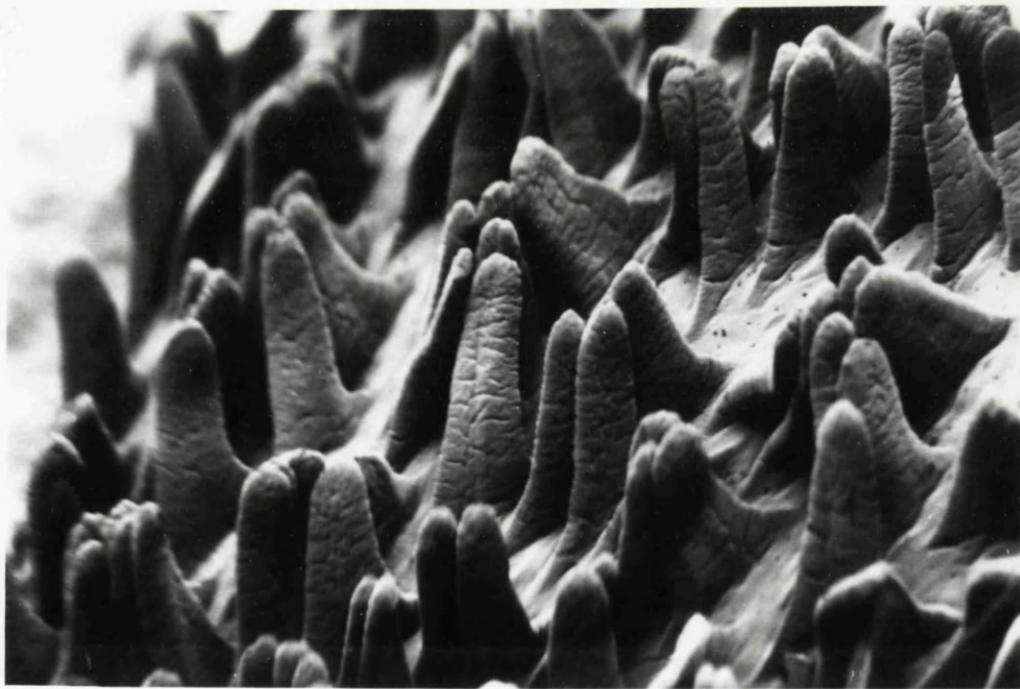


Figure 3.3

SEM of normal mouse *Jejunum* which has been over distended (x100).

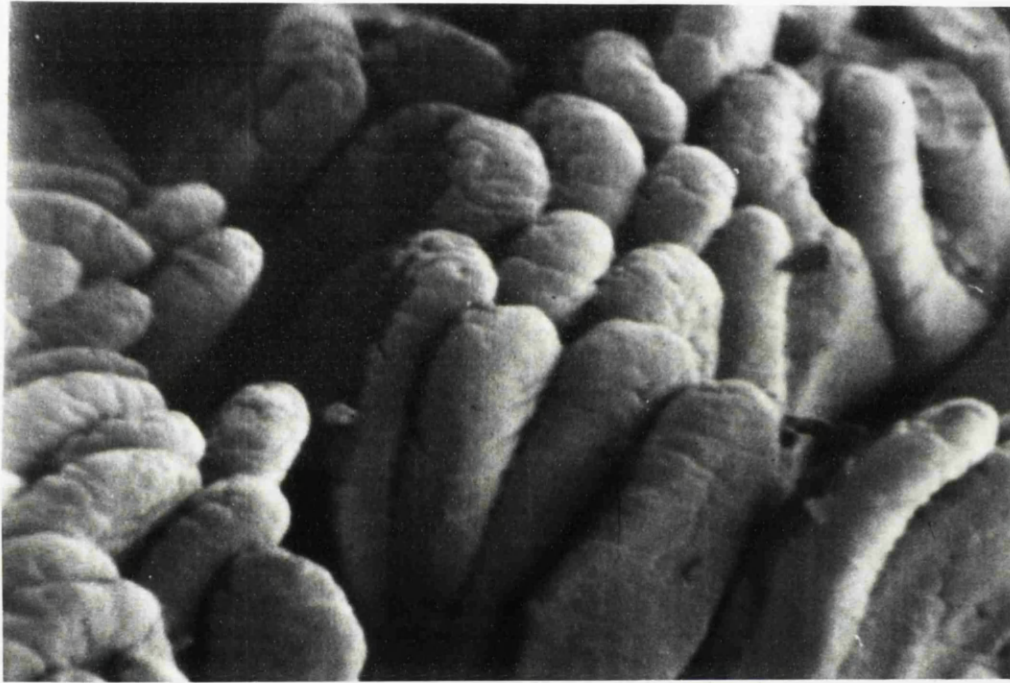


Figure 3.4

SEM of underdistended normal mouse *Jejunum* (x200).

approximately one crypt per circumference) chosen to produce extreme tissue damage and so to maximise the likelihood that specimens would be much more vulnerable to the effects of distension, the following observations were made. In highly distended specimens wider separation of villi were again observed which served to make the surface abnormalities more apparent. However the distension did not, as was feared, increase the mucosal damage already present.

Examination of underdistended specimens from both controls and high dose animals served to demonstrate that in both cases it was extremely difficult to observe the surface morphology with any degree of accuracy. An example is shown in Figure 3.4.

3.6. 'Shoulder' Doses

As stated the first depression of crypt counts occur at 1000 rads for ⁶⁰Cobalt gamma irradiation and 500 rads for D-T neutron irradiation. At these two corresponding points there are clear cut alterations in the mucosal surface as seen by scanning electron microscopy. Gamma irradiated specimens (Figure 3.5) retain the slender villi of the control intestine, but their orientation is inconsistent and groups of villi appear to clump together. Individual villi are more often bent or twisted than those seen in control specimens, the villus tips are often misshapen to a greater degree than their more proximal portions. The

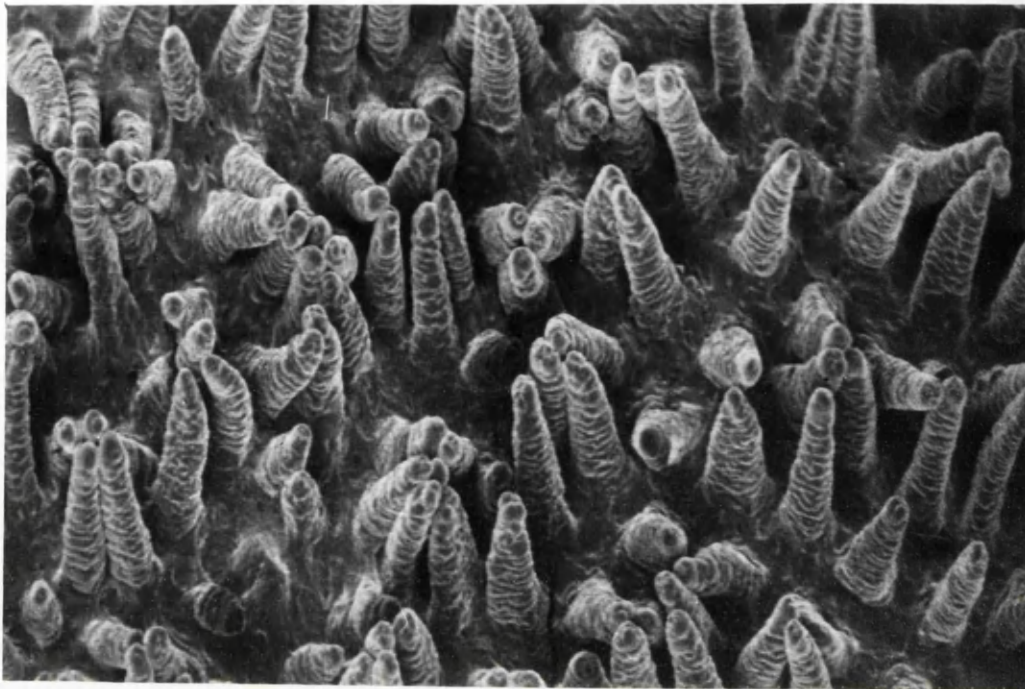


Figure 3.5

SEM of mouse *jejuna* after 1000 rads of ^{60}Co Cobalt gamma irradiation (x100).



Figure 3.6

SEM of mouse *jejuna* after 500 rads of D-T neutron irradiation (x100).

surface creases of the villi, which form in controls an orderly pattern of circumferential grooves, are less consistent in their contours and in their arrangement. Neutron irradiated specimens (Figure 3.6) which show the same relative biological effect in terms of crypt-counts, also show morphological abnormalities. As in the gamma specimens there is an irregularity in the disposition of the surface markings and a change in their nature, these now appear more as rough corrugations of the villus surface than as the linear creases seen in the controls. In addition, neutron damaged villi are consistently more conical in profile than controls and gamma irradiated specimens. Many of the villi are broader at the base and can be described as being of a tongue or leaf shape. This is a marked departure from the morphology as seen in the control mice. Easily distinguished morphological changes therefore, after both types of irradiation, accompany the first quantitative effects demonstrable with crypt counts.

3.7. Higher Doses

Beyond the initial quantitative threshold progressively increasing doses of irradiation produce an exponential fall in the counts of regenerating crypts (see Figure 3.1).

The morphological changes seen by scanning electron microscopy are also progressive. At dose levels which

reduce survival to about ten crypts per circumference with gamma irradiation (1600 rads) the villi retain their initial slender contours, although surface irregularities become progressively more obvious. An example of this is shown in Figure 3.7. Twisted bent and clumped villi are more numerous and marked distortion of the tip of the villus is often seen at times with concave indentations.

After a neutron dose which reduces crypts to an equivalent number (800 rads) the tendency towards flattened and conical villi persists whilst not becoming significantly more marked. The surface contours are strikingly abnormal, the corrugations being no longer largely circumferential but now also vertical (see Figure 3.8). While some specimens show a degree of bending and twisting of the villi, this is a much less striking feature than is seen in the gamma irradiated mucosa. The mucosal changes therefore, whilst dependant to an extent on the type of radiation run parallel to the qualitative changes on the exponential portion of the survival curve, that is, becoming increasingly severe with increasing dose.

3.8. Low Doses

Irradiated specimens which have received doses of less than 1000 rads of gamma or 500 rads of neutron irradiation, have crypt counts which are indistinguishable from those of control specimens.



Figure 3.7

SEM of mouse jejunum after 1600 rads ⁶⁰Cobalt gamma irradiation (x100).



Figure 3.8

SEM of mouse jejunum after 800 rads of D-T neutron irradiation (x200).

Thus any damage that they have received is below the level of discrimination of the crypt counting technique. It was found, however, that observations of damage could be made using scanning electron microscopy.

In the gamma series minor changes in villus orientation could first be made after doses of 300 rads. This dose is approximately one third of that required to produce a significant depression in crypt count. In Figure 3.9 it can be seen that there is a slight distortion at the tips of some of the villi, but there is little change in the surface creases of the villi.

A dose of 170 rads of neutron irradiation also produces minor changes (see Figure 3.10). There is a slight broadening or swelling of the villi and a distinct irregularity of the surface creasing.

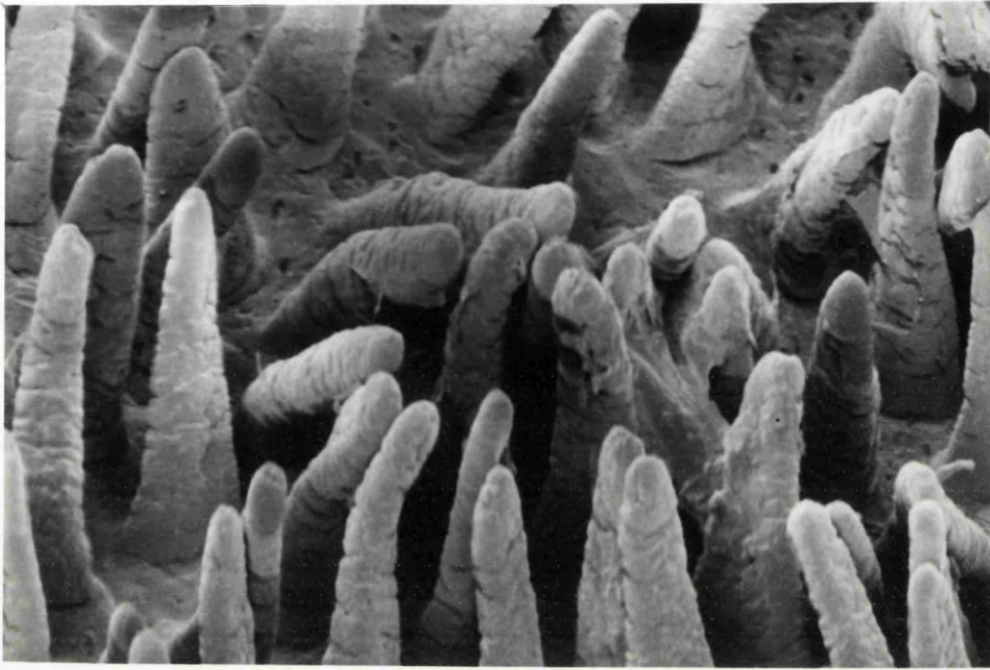


Figure 3.9

SEM of mouse *Jejunum* after 300 rads of ⁶⁰Cobalt gamma irradiation (x200).



Figure 3.10

SEM of mouse *Jejunum* after 170 rads of D-T neutron irradiation (x200).

3.9 Discussion

The results obtained with the regenerating crypt system were qualitatively comparable with previously published work (Withers et al., 1970; Broerse et al., 1971) although D_0 and RBE values were higher. This is possibly due to the fact that a different strain of mice was used in these experiments and ^{60}Co Cobalt gamma irradiation was used, not X-irradiation.

The crypt counting technique gives standardised consistent and easily reproducible quantitative data concerning radiation damage to the stem cell population of the intestinal epithelium by higher doses of radiation. It is, however a relatively insensitive indicator of total mucosal damage. Scanning electron microscopy produces visual results which express this damage in terms of surface changes in the injured mucosa. Qualitative changes such as these are intrinsically difficult to quantitate. However at the lower dose levels commonly used in clinical radiotherapy they are a much more sensitive indicator of damage than is the counting of surviving crypts. The results of these experiments demonstrated differences in the qualitative expression of the mucosal damage resulting from the two forms of radiation used. Although the reasons for this are still not clear it has been found possible to discriminate by scanning microscopy between neutron and gamma irradiation specimens throughout the range of doses covered in the experiments. It would

seem that the many biological variables which contribute to intestinal morphology are independently and differently affected by neutron and gamma irradiation. A possible speculation is that at a given level of radiobiological effect the intense localised ionisation of the neutron beam produces more pronounced effects in vascular epithelial and connective tissue than the diffuse ionisation of gamma irradiation.

The need for standardised tissue preparation techniques has been pointed out by Anderson et al. (1973). The results of the distension experiments confirm these findings. However, it appears that the relatively small variation between specimens that occurs with the inflation technique are unlikely to lead to any serious misinterpretation of the ultrastructural effects of irradiation.

In conclusion, the qualitative technique of scanning electron microscopy provides a more sensitive indicator of mucosal irradiation at low dose levels. There is also good evidence that morphological studies provide a means of discriminating between the effects of low and high LET radiations at dose levels which are radiobiologically equivalent on certain other quantitative scales.

CHAPTER 4

CRYPT SURVIVAL AND SURFACE MORPHOLOGY OF THE GUT
AFTER FRACTIONATED DOSES OF X AND γ IRRADIATION

4.1. Introduction

From the experiments reported in the previous chapter it can be seen that the results of Scanning electron microscopy provide a more sensitive indicator of mucosal irradiation damage at low dose levels than the more conventional qualitative techniques. Similarly it is possible to conjecture that the measurement of the number of surviving crypts after lower doses of fractionated radiation would provide only a relatively small amount of information about the state of the 'functional' apparatus of the gut, the surface mucosa, even after doses of radiation which induce suppression of the cell proliferative system.

As the integrity of the intestinal mucosa is dependent on the continued proliferation of cell systems, a schedule of fractionated radiation which would only slightly reduce total crypt numbers, might produce considerable mucosal disruption. This is because the numbers of viable cells available to enter the maturation pool would be reduced. In order to investigate this possibility experiments were devised in which the biological effect of various fractionated schedules was assayed from the point of view of both crypt regeneration and of the appearance of the surface mucosa.

4.2. The Experiments

Fractionation regimes were chosen using small doses more

relevant to the situation in clinical radiotherapy, where large single doses are rarely delivered. Two of the irradiation schedules were carried out using whole body ^{60}Co Cobalt gamma irradiation and a third using X-irradiation localised to the abdomen.

^{60}Co Cobalt Gamma Irradiation to the Whole Body

Schedule A

Mice were irradiated with 300 rads administered at 24 hour intervals to a total of ten fractions. There was a two day gap between the fifth and sixth fractions over the weekend as is customary in clinical radiotherapy. 24 hours after the final 300 rad dose an 'assay' dose of 900 rads was administered to try and reduce crypt cellularity and hence crypt number to a level which could be counted with accuracy. Each fraction point was investigated; i.e., samples were taken from mice which had received only one fraction or two fractions and so on. This procedure was followed in all three irradiation schedules.

Schedule B

Mice received fractions of 450 rads of gamma irradiation administered at 24 hour intervals.

250 kV X-Irradiation (to the Abdomen Only)

Schedule C

Mice received three fractions of 250 rads daily to a total of 18 fractions in 6 days. The three fractions

were given during the day with a period of three hours between fractions and hence there was an 18 hour period overnight when no irradiation was administered. This 18 hour interval occurred therefore between every third and fourth fraction administered.

RESULTS

4.3. Regenerating Crypts

Figure 4.1 shows the dose-response data for the effect of suppression of crypt numbers for all three schedules. For comparison the curve of the effect of single doses of ^{60}Co Cobalt gamma irradiation is included as a dotted line (reproduced from Hamlet et al., 1976). The curves are all fitted by eye and because there is no significant difference between the crypt counts of all three schedules over the range of the first 2000 rads, a common line was drawn. This common line also happens to be the best fit for the whole of the data from Schedule A.

The controls for all the experiments have a mean value of 122 ± 10 crypts per circumference. There is a fall to 96 ± 12 crypts after a total dose of 3,900 rads with Schedule A. Schedule B produced a greater reduction to a mean count of 85 ± 5 crypts after a total dose of 2,250 rads and Schedule C a fall in crypt count to a mean level of 18.5 ± 6 crypts after a total dose of 4,250 rads.

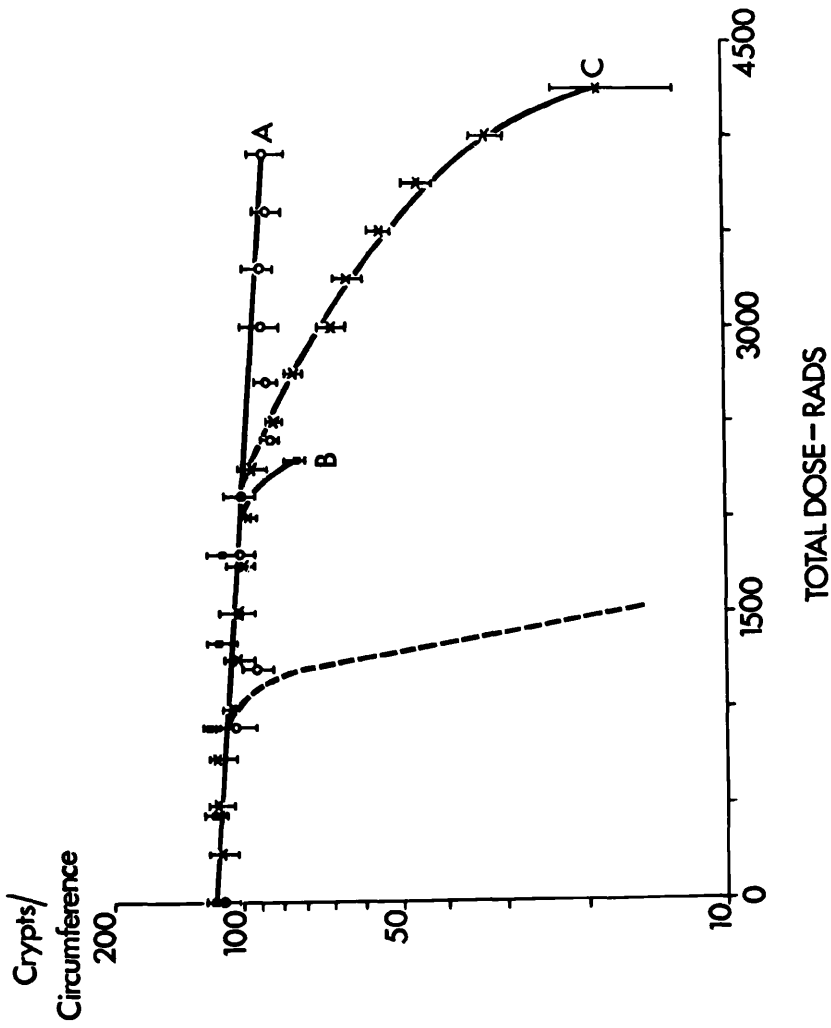


Figure 4.1
 Crypt survival curves for Schedules A, B and C and single dose of ⁶⁰Cobalt gamma irradiation (dotted line).

4.4. Presentation of Crypt Data

Hendry and Potten (1974) have shown that regenerating crypts three days after single doses of irradiation appear larger than normal crypts. Thus they would have a greater probability of appearing in a section of intestine. For accurate assessment of D_0 and extrapolation number, particularly after crypt survival data is transformed into values of cell survival, they suggest that a correction factor of 0.88 be applied to crypt results obtained from irradiated intestine. As it was found that in these experiments there was no significant difference between crypt counts from control animals and that given low doses, and because a conversion to cell survival is not used and also because the crypt results are being used principally for comparison between fractionation schedules, it was decided that it is not necessary to use a correction factor for the presentation of the crypt survival data from these experiments.

4.5. Animal Condition and Postmortem Observations

Because the schedules involved either whole or partial body irradiation particular attention was paid to the general condition of the experimental animals.

Postmortem examinations were made on all animals dying before the day of assay, which was always $3\frac{1}{2}$ days after the final irradiation dose. The health of the irradiated mice varied depending on the schedule and

the total dose administered. All the animals were in excellent condition at the beginning of the experiments and those receiving a small number of fractions remained healthy. After larger numbers of fractions the condition of the animals deteriorated. It was in these groups that some early deaths occurred. A description of the health of the animals and postmortem observations for each schedule are given below.

Schedule A

These animals which received the higher numbers of fractions were in poor condition at the end of each experiment. They showed considerable weight loss and on postmortem examination the intestines contained only fluid and were often distended with gas. The intestinal walls were usually stained dark green and were rather fragile. Deaths occurred in groups receiving 8 to 10 fractions. Postmortem examination revealed that these animals had extreme intestinal damage, but also showed signs of bone marrow failure. Petechial haemorrhages of the skin and intestinal mucosa were always present and large haemorrhages were often observed. Thus the relative contribution of these two types of radiation injury toward the actual cause of death in each individual mouse was very difficult to determine.

Schedule B

All the animals remained in good condition, up to a total of five fractions of 450 rads and on examination their organs all appeared to be in reasonable condition.

However, if six or more fractions were administered all of the animals died before the day of assay. This was presumed to be due to bone marrow failure since serious haemorrhage was always observed at postmortem.

Schedule C

The animals receiving nine or more fractions of 250 rads three times per day deteriorated in condition over the period of experimentation. All the animals which received 18 fractions died and there were some deaths in each of the groups of animals which received 13 or more fractions. On postmortem examination all of the animals showed severe damage to the intestinal tract including distension of the intestines with fluid and gas with considerable staining of the intestinal walls. In no case was it possible to discern signs of bone marrow failure.

4.6. Scanning Electron Microscopy

The results of Scanning microscopy show that in all the schedules there is an unevenness of the progression of surface damage with increasing dose and in a small number of cases a variation in the damage seen in specimens from different animals which had received the same total dose. There was some variation in the appearance of control specimens. In addition there were some features of gut morphology seen from one of the experiments in Schedule C which had not previously been observed in irradiated animals.

4.7. Damage Assessment Using Scanning Electron Microscopy

In order to try and assess these results seven different factors influencing the morphology of the villi were chosen and the micrographs for each piece of gut were assessed independently for each of these factors.

These factors are:- Apparent villus height, apparent width, separation of the villi, contours of the villus tips, erectness of the villi, clumping of the villi and finally creasing of the villus surface with accompanying surface damage which can be described as wartiness or blebs. Each of these factors was scored on a ranking system from 1 to 8. 1 representing the real or 'ideal' appearance as would be seen in a well preserved control specimen. 2 and 3 represent minimal or slight damage, 4 and 5 indicate moderate to substantial damage and 6 to 8 to indicate severe to gross damage. The mean scores for each factor were obtained from the scores from individual specimens. For any given dose, the mean scores for all the factors were then added together to give a total which could be used as an index of cumulative damage. A compound histogram was then constructed, providing a graphic and semi-quantitative representation of the morphological variations with increasing dose and including the controls. It can be argued that these factors or parameters have been only subjectively assessed. However, the problems raised by disorientation, twisting and banding of the villi which occur at higher dose levels are such that at the present

time Scanning electron microscopy cannot be used for accurate quantitative measurements. In fact the difficulties are such that even conventional histological specimens could not be *quantitatively assessed for* surface damage and are considered to lie beyond the scope of this investigation. Certainly the same subjective assessment of the Scanning electron micrographs was made for all the aspects of damage, and this treatment ensures that assessment of damage is less biased towards any individual factor.

The compound histograms for the three schedules are shown, with the relevant crypt count graph in Figures 4.8, 4.9 and 4.10. The doses illustrated by the Scanning electron micrographs in Figures 4.4 to 4.6 are marked on the crypt count graphs. This allows the individual micrographs to be examined in context with the damage observed throughout the schedule, as seen by crypt counting and scanning microscopy. The damage seen by scanning microscopy as interpreted through the histograms is described below for each schedule with a separate section dealing with the normal variations observed in control specimens.

4.8. Controls

Two examples of mucosa from untreated mice are shown in Figures 4.2 and 4.3 for comparison with the micrographs obtained of specimens from irradiated animals. It can be seen that there are variations in the appearance of

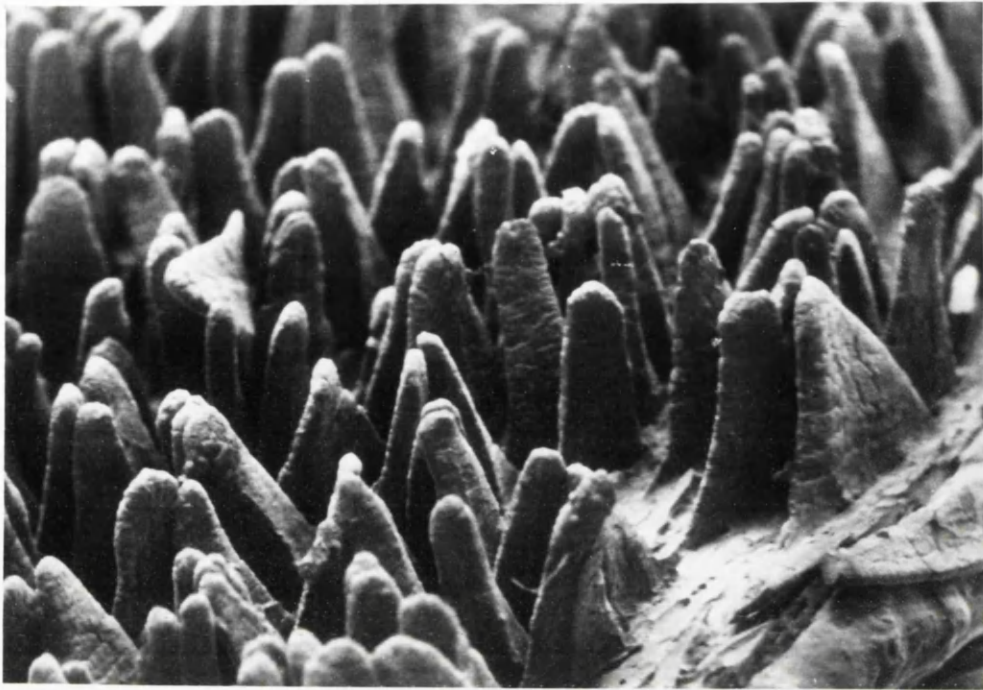


Figure 4.2

SEM of control specimen. A good quality control showing well defined finger like villi (x100).

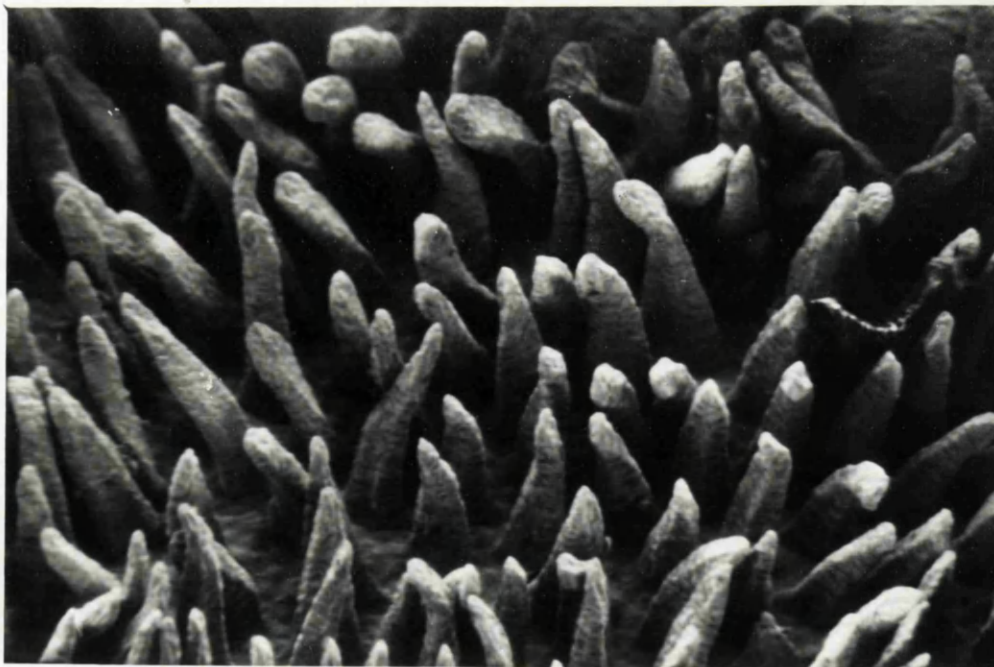


Figure 4.3

SEM of control specimen chosen for its relatively poor quality (x100).

the villi of control specimens but these variations are relatively slight and not comparable with the type of damage seen in micrographs of gut taken from irradiated mice. Using the SEM scoring system figure 4.2 scores 7 (the lowest score for an ideal control). Figure 4.3 scores 9 which is slightly higher but well below the values of 15-30 which were achieved with irradiated specimens. The main difference between these two control specimens is that the villi in the second picture (Fig. 4.3) are less erect than in the other sample (Fig. 4.2) but their other characteristics are *VERY SIMILAR.*

To illustrate the conclusions of this work, and to save space one photograph has been chosen from each of the fractionation schedules. A more detailed appreciation of the results can be obtained by examining the histograms in the later figures (4.8 to 4.10) and will make clear how representative these pictures are.

4.9. SEM Damage Assessment in the Three Schedules

Schedule A

Figure 4.4 shows a specimen of mouse intestine from Schedule A, which came from an animal which had received a total dose of 3000 rads (7 fractions of 300 rads + 900 rad assay dose). The specimen had a mean crypt count of 95 and a mucosal damage score of 30. Figures 4.8A and 4.8B demonstrate that Schedule A, although producing

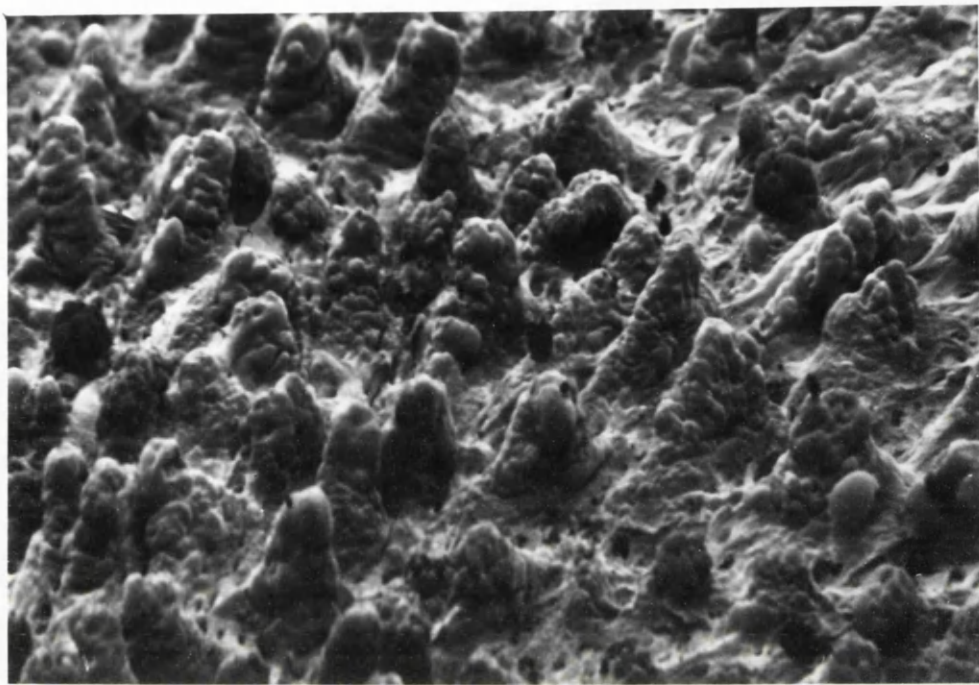


Figure 4.4

SEM from Schedule A, of a specimen which received a total dose of 3000 rads (7 fractions plus assay dose). The villi are badly damaged (x100).



Figure 4.5

SEM from Schedule B, of a specimen which received a total dose of 2250 rads (5 fractions). The villi appear longer and floppy but are not badly damaged (x100).

only a small depression in crypt number, brought about considerable disruption of the intestinal mucosa.

Schedule B

Figure 4.5 shows a specimen from Schedule B which had received a total dose of 2250 rads (5 fractions of 450 rads). It achieved a mean crypt count of 85 and a score for mucosal damage of 13. The villi are clumped together and less erect than controls. They appear however, to have a slightly greater than normal height, but are not badly damaged. An examination of Figures 4.9A and 4.9B shows that a small depression in crypt count is correlated with a small amount of villus damage with this schedule. There is a greater degree of damage reflected in the crypt count after five fractions in Schedule B than after 11 fractions in Schedule A, despite the fact that a smaller number of fractions and a lower total dose were administered. But it must be remembered that the individual fraction size was $1\frac{1}{2}$ times larger. In comparison, Scanning microscopy showed that surface damage was less severe than that produced by Schedule A. The histogram in Figure 4.9B demonstrates that there is not much increase in damage after the initial rise observed after the first fraction. These observations can permit speculation into the possibility of there being a dose/threshold effect but as yet the evidence is inconclusive.

Schedule C

With Schedule C there is a good correlation between the results of the two assay methods. Figure 4.6 shows a specimen with a very badly damaged mucosal surface after a total dose of 4,250 rads (17 fractions of 250 rads). This specimen had a mean crypt count of 18.5 and a mucosal damage score of 24. Figures 4.10A and 4.10B show that both crypt counts and surface morphology reflect evidence of progressive increase in damage with increasing total dose. As in the two other schedules the changes in mucosal morphology are more variable than the crypt counts. Marked mucosal damage is seen with stumpy and deformed villi with 11 or more fractions, as demonstrated in Figure 4.6. The assessment of the damaged samples was complicated by the presence of *mucus* which is often seen after heavy irradiation. The observations of low crypt count and high mucosal damage after high total dose that have been made with this schedule, are completely at variance with the results obtained after Schedule A. In the latter case high crypt count being correlated with severe mucosal damage.

An interesting feature of the experiments pertaining to Schedule C was the appearance of villi with a marked leaf or ridge shape in some specimens which had received 17 fractions of 250 rads. This has been observed in irradiated rats (Anderson and Withers, 1973) but has not previously been seen to occur in any mouse irradiation

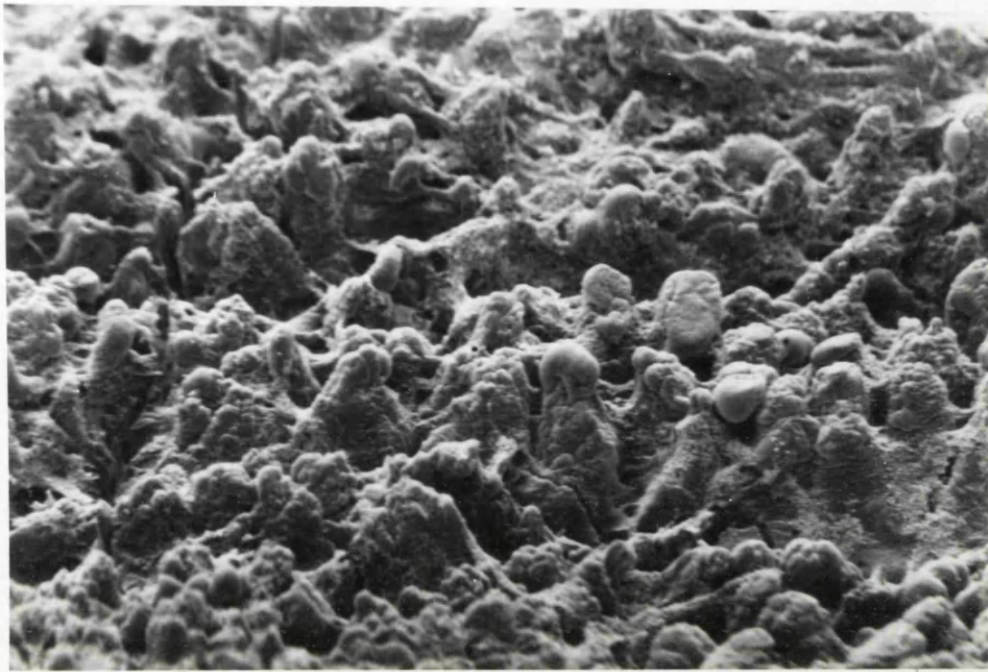


Figure 4.6

SEM from Schedule C, of a specimen which received a total dose of 4250 rads (17 fractions). The surface mucosa is very badly damaged (x100).

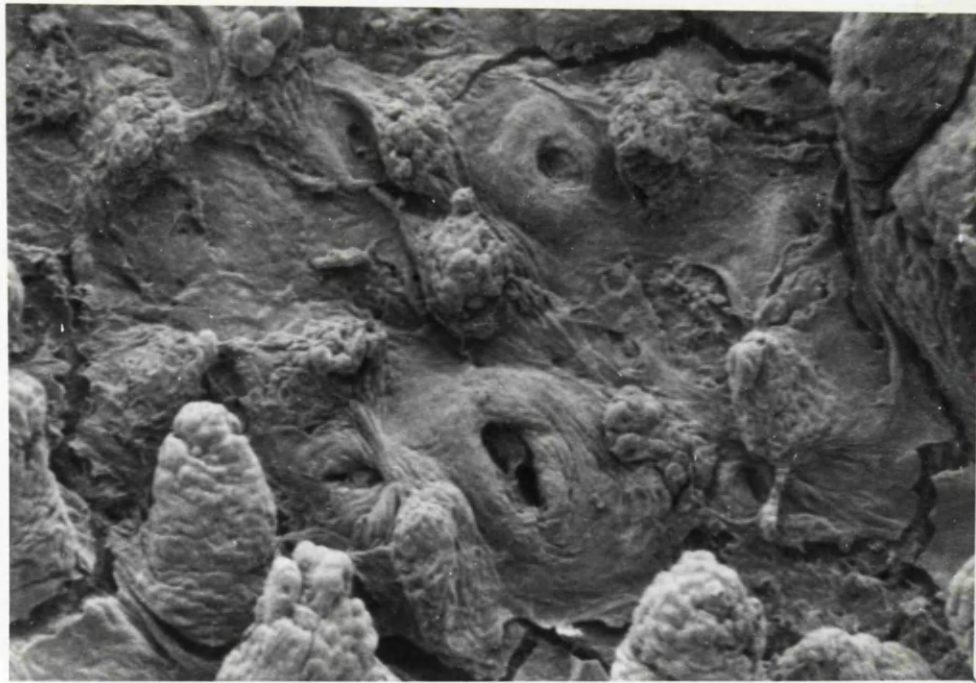


Figure 4.7

SEM from Schedule C. Total dose 3750 rads (15 fractions) showing morphology similar to that seen with human coeliac disease (x200).

experiments. There were also three samples from the Schedule C experiments, which had received 11, 13 or 15 fractions, showing a patchy abnormality consisting of a localised absence of villi and a heaping up of cells around the crypt mouths. Figure 4.7 shows a sample of irradiated gut showing these changes. This pattern is similar to that of human coeliac disease and has not been seen in previous irradiation experiments (Carr and Toner, 1972).

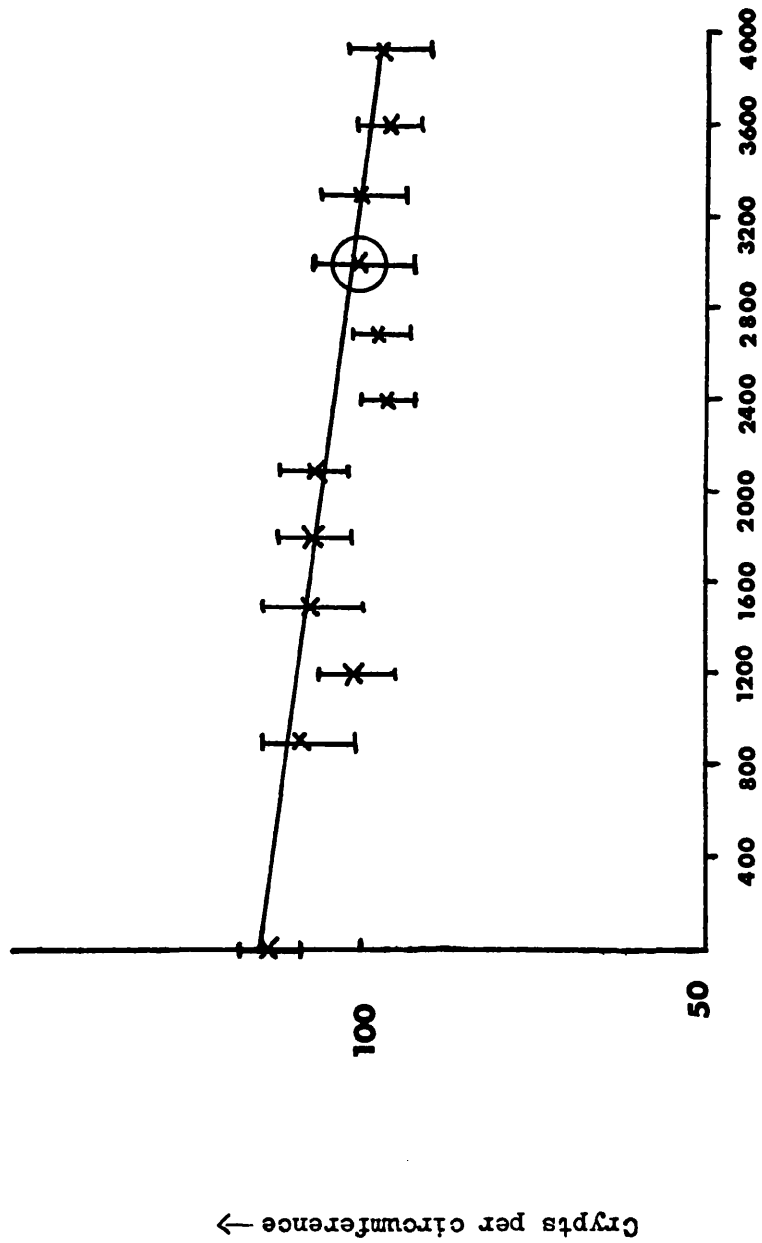
4.10. Discussion of Results

The intestine is so radiosensitive that even a few low dose fractions will reduce crypt cellularity. Crypt numbers, however, will not be affected until the number of cells in any particular crypt has been reduced to less than one. As in theory one remaining crypt cell is sufficient to regenerate a crypt, or rather a clone of crypt cells, within a period of three to four days. It follows that the response to radiation will be seen initially in the crypts followed in due course (depending on the transit time) by a reduction of villus cell population and therefore of villus height. It would therefore be expected that a fractionation schedule extending over a period of time much in excess of the transit time of the intestinal cell population from crypt to villus tip would effect a situation whereby the extent of crypt damage would be reflected in the amount of villus damage and vice versa. This

expectation was confirmed by the data from treatment Schedule C but not with Schedule A and only to a small extent with Schedule B.

In Schedule A, animals which received 7 or more fractions have crypt counts only slightly lower than control values but have mucosal surfaces which show considerable abnormality (see Fig. 4.4). It is doubtful if these animals, which show such severe mucosal damage, could absorb sufficient food and fluid or maintain an adequate electrolyte balance (Jackson et al., 1958; Curran et al., 1960) to survive until the large numbers of surviving cells in the crypts could effect repopulation of the mucosal surface.

This phenomenon of high crypt count with severe mucosal perturbation may be explicable in terms of cell population kinetics (as outlined by Hagemann et al., 1975 and Hagemann, 1976). If one supposes continued cell proliferation in the crypts which are receiving repeated radiation insults, it is possible that there are insufficient viable cells moving into the maturation stage, thus resulting in a reduction of the number of mature functional cells arriving at the villus. This, combined with the normal loss of cells from the extrusion zone, might result in the type of damage seen in Figure 4.4. The variation in damage seen throughout the series of samples from this schedule (as demonstrated in the histogram in Figure 4.8B) is more difficult to explain and is probably of multifactorial origin. It is



Total dose in rads →

Figure 4.8A

Crypt survival curve for Schedule A. Circle refers to the sample shown in figure 4.4.

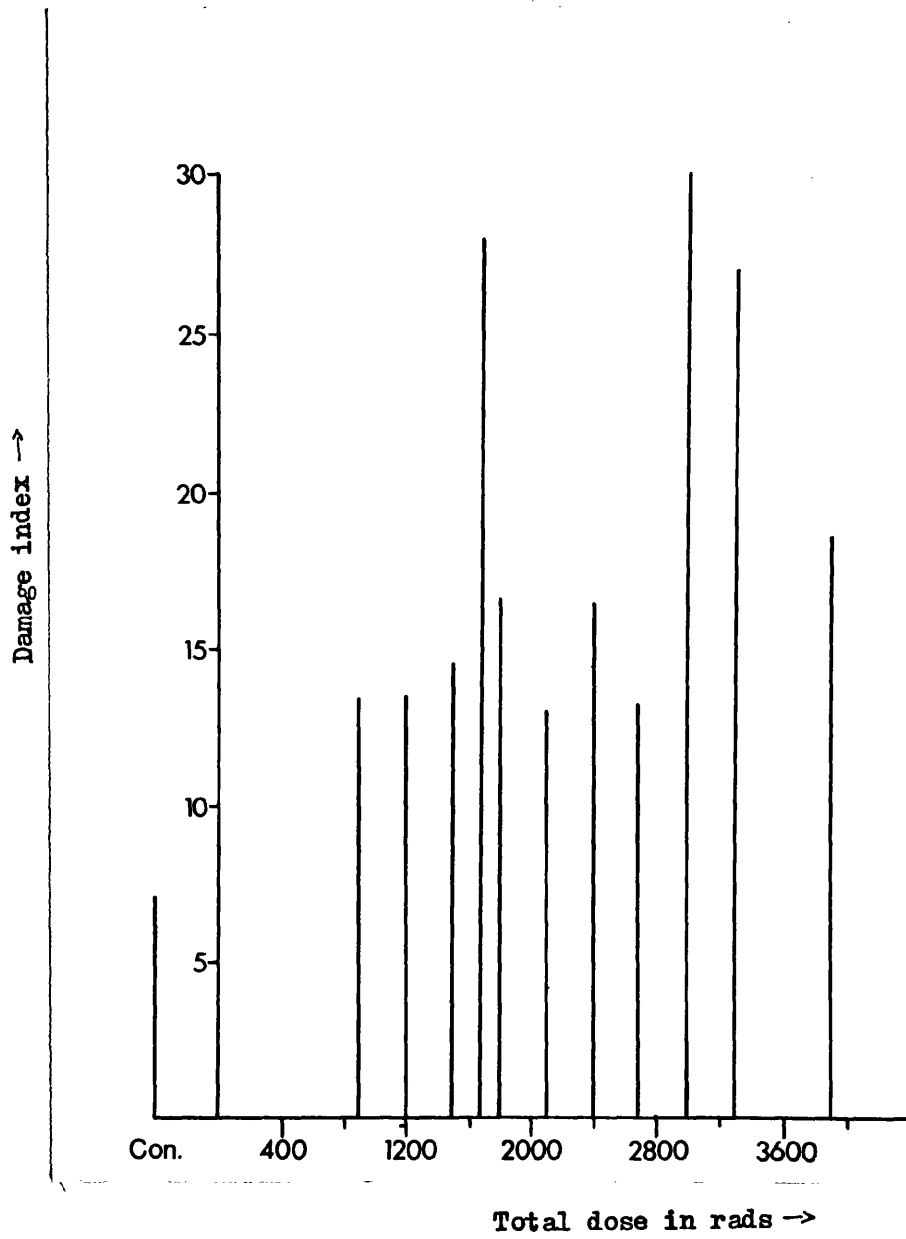


Figure 4.8B

Histogram of surface damage in Schedule A as illustrated by scanning electron microscopy.

almost certain that cellular repair and repopulation particularly over the period of the two day gap in the middle of the schedule and the relatively large 'assay' dose all have a part to play in bringing about the interseries variation.

Schedule B resulted in a significant fall in crypt number to a mean of 85 ± 5 . This was associated with the observation of only a moderate amount of damage to the surface mucosa. The differences from Schedule A can probably be attributed to the following factors. First, the individual fraction size is considerably higher, and although no 'assay' dose was used in these experiments the larger fraction size might be expected to produce a greater net reduction in crypt cellularity. Secondly, the experiments were of much shorter duration than those in Schedule A because of the high incidence of bone marrow death with increased total dose. If the schedule could have been continued further, there would have been more time for loss of cells from the extrusion zone of the villus, and thus more pronounced mucosal damage would have been expected to appear at a later time. It is also possible to conjecture that the 'floppy' appearance of the villi as seen in Figure 4.5 could be due to the underlying connective tissue and vascular frame-work rather than to the cells of the epithelial system.

Schedule C resulted in a much better correlation between the reduction in crypt numbers and increase in

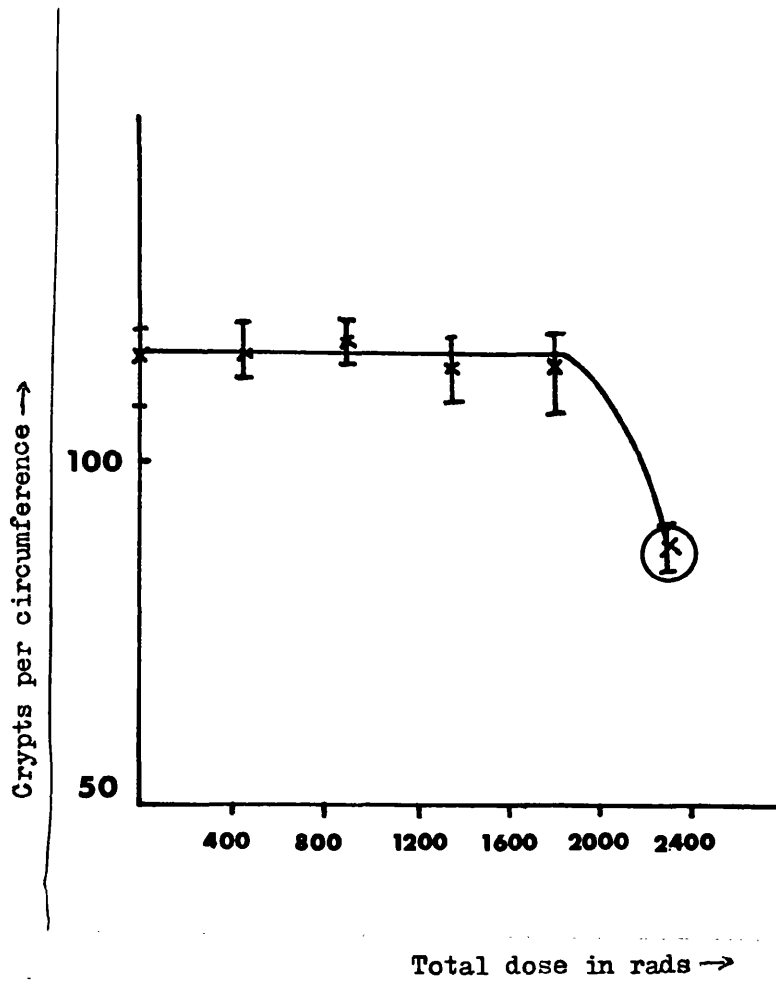


Figure 4.9A

Crypt survival curve for Schedule B. Circle refers to sample in figure 4.5.

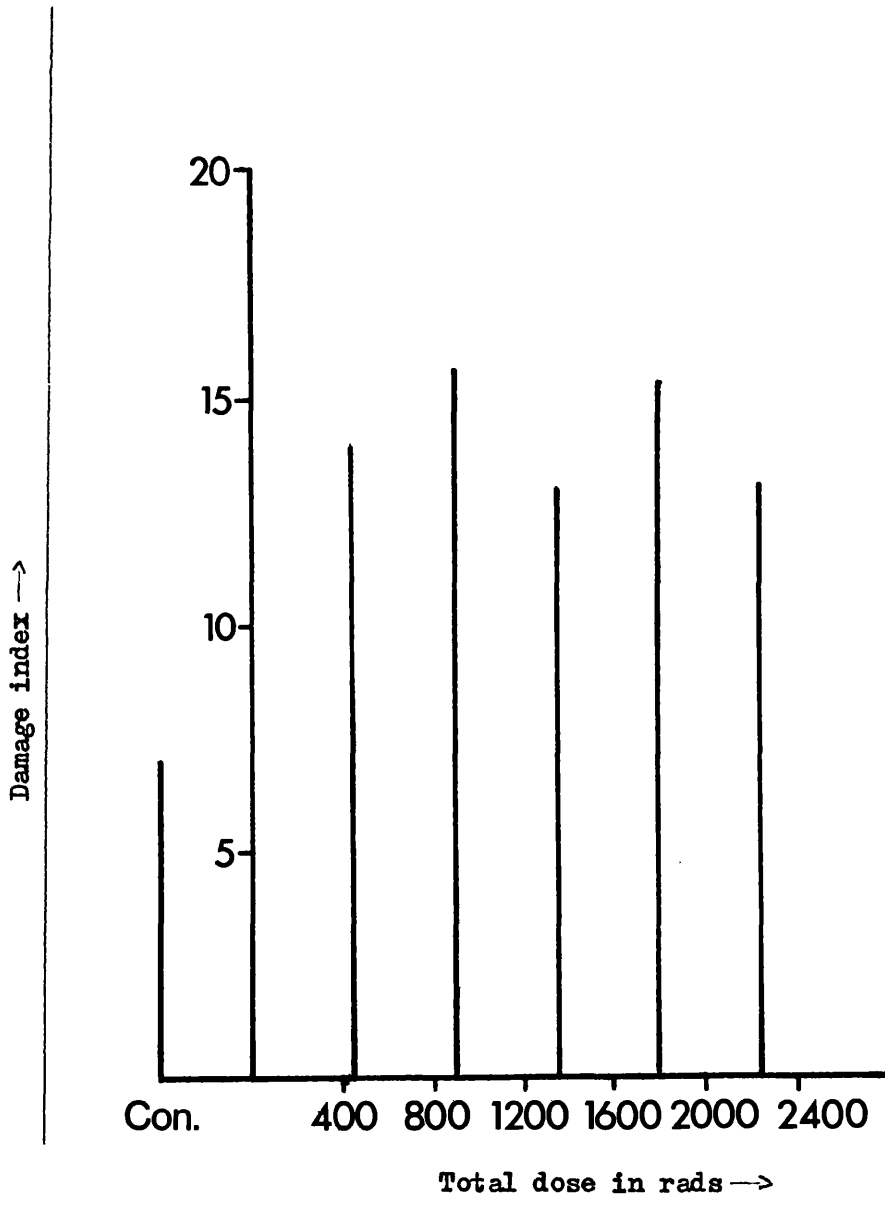


Figure 4.9B
 Histogram of surface damage in Schedule B.

mucosal damage (see Figs. 4.10A and 4.10B). The increased number of fractions administered (three fractions per day) and the consequent decrease in the duration of the interval between fractions produced a much greater reduction in crypt cellularity. This brought about a fall in crypt number and severe damage to the surface mucosa due to the small numbers of cells available to maintain mucosal integrity. Variations in mucosal damage in this series (see Fig. 4.10B) are probably attributable to repopulation occurring during the relatively long gap of 18 hours between each third and fourth fraction. Thus, although surface morphology may indeed be a sensitive indicator of radiation injury of the mucosa its interpretation in terms of the perturbation of cellular kinetics can be extremely difficult. For example, it is not possible to explain the appearance of mucosal damage similar to that seen in human coeliac disease (see Fig. 4.7), since in theory at least, the kinetics should be widely different.

Much of the radiobiological literature concerning the radiation response of the small intestine is based upon the microcolony assay system of Withers and Elkind (1970). Use of this system has provided detailed dose-response data for both single and fractionated radiation schedules (Withers et al., 1975) and the assumption has been made that the response of the jejunal mucosa is dependent upon the capacity of crypt stem cells to repair sublethal damage and to regenerate. This

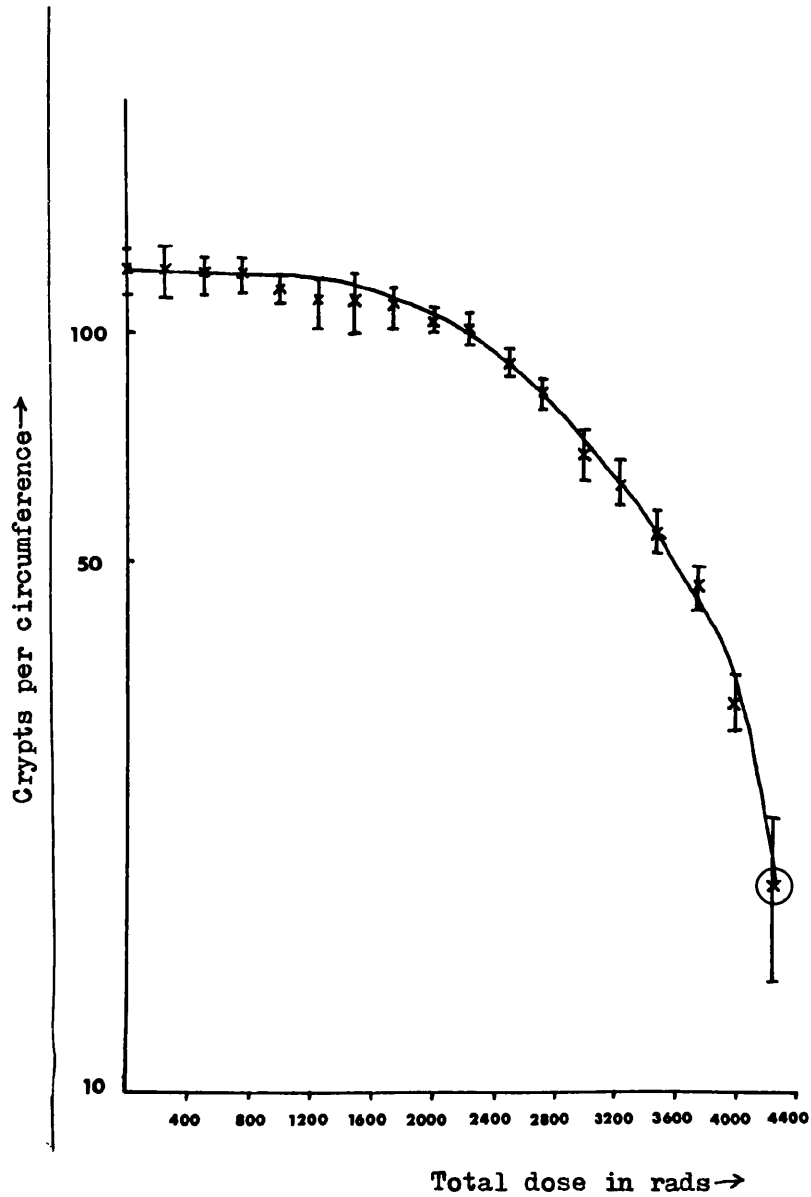


Figure 4.10A

Crypt survival curve for Schedule C. Circle refers to sample in figure 4.6.

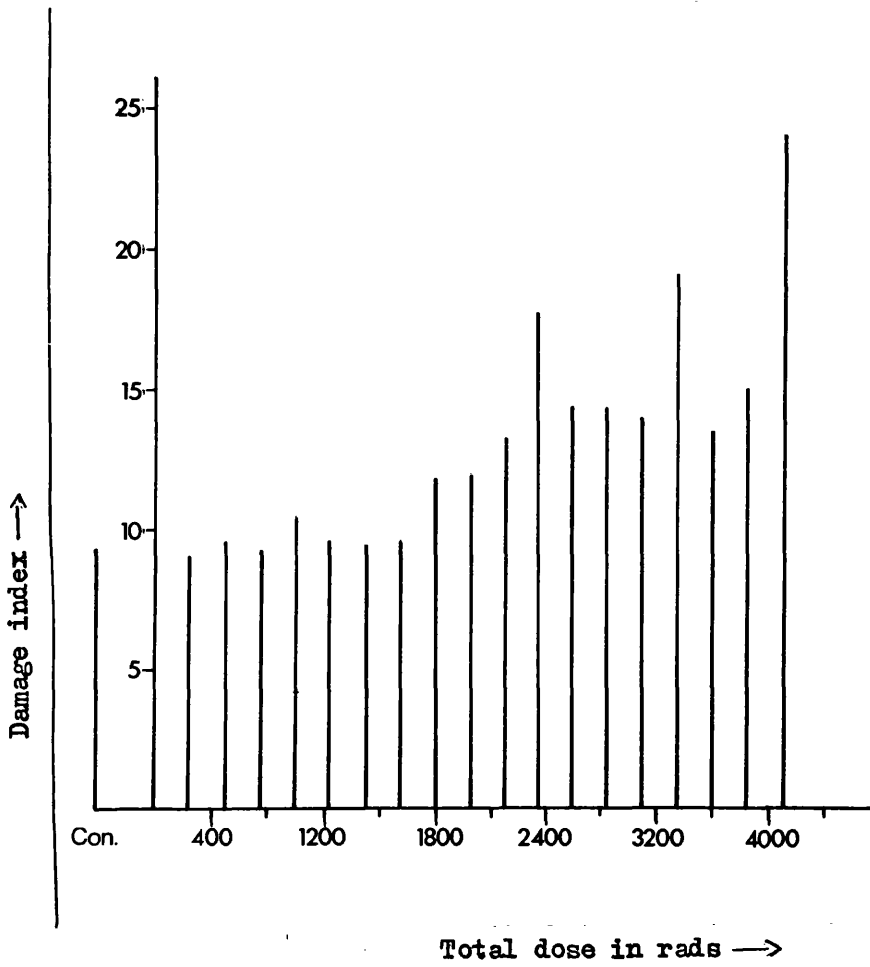


Figure 4.10B

Histogram of mucosal damage in Schedule C.

hypothesis has been confirmed by experiments (carried out by the previously mentioned authors) where mice received 275, 300 or 325 rads per day for 9 days and a final dose of 1230 rads on the tenth day. (A similar regime to Schedule A). They concluded that crypt cell numbers were probably not depleted after such a regime. These authors make no observation on the effect on the villus surface of such a regime, *but concluded that the* lethal effects of villus denudation are assumed to correlate with severe crypt damage but the present studies show that this may not always be the case. The alternative end point of gastrointestinal death does not necessarily provide a correlation either (Wambersie et al., 1974). This is because such data, based upon the simple end point of death or survival, does not permit much resolution of the degree of damage to the mucosal surface. The majority of studies have been concerned with the acute effects of radiation on the gut. However, late complications of radiotherapy have also been reported (Roswit et al., 1972) and it has been shown that late changes may mimic the effects of malabsorption syndromes (Wellwood and Jackson, 1973).

Thus the experimental results and the data from the literature confirm the importance of damage to the intestinal mucosa in limiting the dosage of radiotherapy delivered in various fractionation regimes. They also emphasise the fact that doses which do not seriously disturb the proliferative capacity of a biological

system might considerably disrupt its specific function. This in turn might effect systems remote from the site of injury. The results also demonstrate that damage to different sections of the same organ may develop at different times thus complicating the complete picture of radiation injury.

CHAPTER 5

A BIOLOGICAL INVESTIGATION OF THE ALTERNATING
FRACTIONATION FORMULA OF THE CRE MODEL

5.1. Introduction

Two predictions arise from the CRE model in connection with alternating fractionation schedules. The first is that the alternation of two fractions of different sizes within an irradiation schedule will produce a greater biological effect than the repetition of a single sized fraction provided that the fraction interval, number of fractions and total dose are the same in both cases (Kirk, 1975). For example if five fractions of 450 rads and five fractions of 150 rads are administered alternately at daily intervals to a normal tissue, the effect on that tissue will be greater than that produced by 10 daily fractions of 300 rads, although the total dose (3000 rads), fraction interval and number of fractions (10) are the same in both instances.

The second prediction of the formula is that the order in which the alternate fractions are given will have no effect on the biological end point as long as the other schedule parameters are adhered to in all cases. Thus if all the fractions of 450 rads were administered before all of the 150 rad fractions the resulting biological damage should be the same as that produced if all the 150 rad fractions were given before all the 450 rad fractions. Similarly, the damage would be the same as that produced when each individual fraction was alternate (Kirk et al., 1971). Experiments were designed to investigate these two theoretical predictions of the CRE model.

5.2. The Experiments

In all the experiments the mice were irradiated with whole body doses of ^{60}Co Cobalt gamma irradiation. The type of schedule used was three fractions given at three hour intervals with an 18 hour interval between each third and fourth fraction. This schedule was chosen as it was known to produce a significant reduction in crypt numbers during the period of administration of the irradiation fractions, but also because of its relevance to the type of schedule in clinical use at some centres at the present time.

Assay was of the mean number of surviving intestinal crypts per circumference, three and a half days after a given number of fractions were administered.

Assay was made after each fraction in the standard schedule experiments and after every other fraction in the experiments with alternating fractionation schedules as the CRE formula is only valid for even numbers of doses. Unirradiated controls were sampled at the same time as the final assay point in each schedule. In all the experiments a minimum of eight mice were sampled at each individual fraction assay point.

The individual experiments were as follows:-

5.3. The Standard Schedule. 300 rads per fraction were given three times per day up to a total of twelve fractions.

Alternating Fractionation Schedules. Two basic types of experiments were performed but in all of the experiments the fractions were always one of two sizes.

Schedules A and B. Each individual fraction was alternated up to a total of twelve fractions, so that the total dose after even numbers of fractions was the same as in the standard schedule. Thus in Schedule A mice received 150 rads as a first fraction, 450 rads as a second, 150 rads as a third and so on. Schedule B was similar but started with 450 rads as a first fraction.

In Schedules C and D all the fractions of one size were given before all of the fractions of alternate size, up to a total of twelve fractions. Thus in Schedule C all of the 150 rad fractions were given first, followed by all of the 450 rad fractions. Conversely, in Schedule D all of the 450 rad fractions were administered before all of the 150 rad fractions. So that, for example, in Schedule C, mice would receive from one to six fractions of 150 rads followed by one to six fractions of 450 rads. In each case mice were assayed $3\frac{1}{2}$ days after the appropriate number of fractions had been given, (ie 2, 4, 6 and so on up to 12 fractions).

For ease of reference the schedules are summarised in Table I.

TABLE I

<u>Schedule</u>	<u>Treatment strategy (fraction sizes in rads)</u>
Standard schedule	300 + 300 + 300 + 300 - - - - - + 300
{ Schedule A	150 + 450 + 150 + 450 + 150 - - - - - + 450
{ Schedule B	450 + 150 + 450 + 150 + 450 - - - - - + 150
{ Schedule C	150 + 150 + 150 - - - + 150 + 450 + 450 + 450 - - - + 450
{ Schedule D	450 + 450 + 450 - - - + 450 + 150 + 150 + 150 - - - + 150

5.4. Results

Animal Deaths

Because the irradiation was delivered to the whole body some animals died of bone marrow failure before the day of assay. Confirmation of the cause of death was sought from postmortem examinations.

In the Standard Schedule experiments (300 rad fractions) only the animals receiving 12 fractions died before they were due to be killed. In Schedules A and B all the mice which received 10 or 12 fractions died. In Schedule C no animals were lost, but in Schedule D animals which received 12 fractions died before the time of assay. All of the dead animals showed signs of bone marrow failure on postmortem examination.

Crypt Counts

The crypt survival data for all of the experiments is contained in Table II along with the appropriate standard errors. However, for ease of comparison these results are plotted graphically in Figure 5.1. All the lines in this figure have been fitted by eye.

A study of Figure 5.1 shows that the experimental data obtained can be fitted to three discrete lines. Line 1 is fitted to the points obtained with the experiments in the Standard Schedule of 300 rads per fraction. Line 2 is fitted to the points obtained from Schedule C and D and line 3 is fitted to the points obtained with Schedules A and B. It is apparent that

TABLE II

Results of the schedules expressed as mean numbers of surviving crypts per circumference with standard errors.

<u>Crypts per circumference</u>	<u>Standard schedule</u> <u>Total dose (rads)</u>	<u>Number of fractions</u>
124.9 ± 2.7	0	0
120.0 ± 3.4	300	1
120.6 ± 2.0	600	2
118.3 ± 8.1	900	3
117.6 ± 8.1	1200	4
114.0 ± 2.8	1500	5
107.2 ± 5.1	1800	6
98.2 ± 1.1	2100	7
85.2 ± 1.0	2400	8
64.2 ± 1.6	2700	9
48.3 ± 6.1	3000	10
26.3 ± 1.1	3300	11

Schedule A.

<u>Crypts per circumference</u>	<u>Number of fractions</u>	<u>Total dose (rads)</u>
118.6 ± 2.3	0	0
106.7 ± 1.4	2	600
87.3 ± 2.2	4	1200
64.7 ± 2.4	6	1800
43.3 ± 3.1	8	2400

Schedule B.

<u>Crypts per circumference</u>
124.0 ± 1.7
110.2 ± 2.9
92.0 ± 1.4
61.3 ± 1.5
46.4 ± 1.7

Schedule C.

<u>Crypts per circumference</u>	<u>Number of fractions</u>	<u>Total dose (rads)</u>
122.1 ± 0.9	0	0
117.5 ± 1.3	2	600
111.5 ± 1.0	4	1200
82.2 ± 2.4	6	1800
56.5 ± 1.3	8	2400
33.0 ± 1.0	10	3000
12.4 ± 1.2	12	3600

Schedule D.

<u>Crypts per circumference</u>
121.1 ± 1.2
114.8 ± 1.6
94.8 ± 1.8
89.2 ± 1.1
60.4 ± 2.4
32.4 ± 1.4

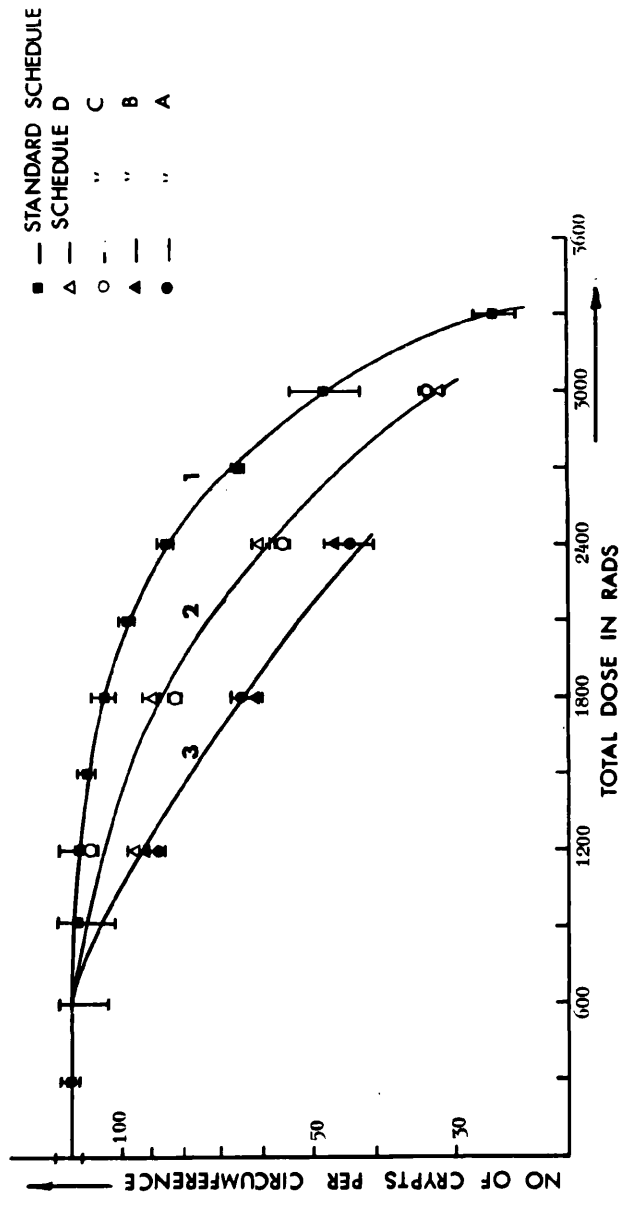


Figure 5.1
Crypt survival curves for the standard and alternating fractionation schedules.

there is a significant difference between the lines at total doses in excess of 1500 rads.

5.5. Discussion

The alternating fractionation formula of the CRE model predicts a greater biological effect from an alternating fractionation schedule than that obtained from a schedule where the fraction size is constant, given that the parameters of total dose, number of fractions and fraction interval are the same. The experimental results are in general agreement with this prediction in that a greater effect was obtained with all four Alternating Schedules. As can be seen in Figure 5.1 lines 2 and 3 show lower crypt counts for the same total dose than does line 1 which is fitted to the results obtained from the Standard Schedule experiments.

However, the formula also predicts that this effect will be independent of the order in which the fractions are administered. Thus the results obtained from the four Alternating Schedules would appear to be at variance with this prediction. If the predicted results had been obtained the results from all four Alternating Schedules would have fitted a single line. In other words, lines 2 and 3 in Figure 5.1 would have been superimposed upon each other. In actual fact line 3 demonstrates that Schedules A and B produced an even greater effect than Schedules C and D (line 2).

It is difficult to explain why these differences

and similarities have occurred. It is doubtful whether this is an effect characteristic only of gut tissue as the observations are to some extent reflected by the higher number of bone marrow deaths which occurred with Schedules A and B. (Those schedules which produced the greatest amount of gut damage.)

Using a simple theoretical consideration of cell proliferation kinetics, which assumes an exponential growth of surviving cells after a dose of irradiation and a constant rate of proliferation between fractions for all the schedules, it can be argued that all the Alternating Schedules should produce the same effect in terms of the total number of cells killed in a given time. Factors such as mitotic delay and the possible effects of synchrony may have a part to play in the explanation of the observed differences between the schedules but it is not possible to say how much influence these factors might exert on the population of regenerating cells. It is also possible that, after a relatively low dose of irradiation, such as 150 rads, repopulation would rapidly make up cell loss even if many of these low doses were administered, but with a larger dose (450 rads) depopulation would occur. This mechanism might explain how in Schedules C and D repopulation might be sufficiently rapid to more than replace lost cells during the period of time when the 150 rad fractions were being administered; whilst in Schedules A and B the interval between each 450 rad

fraction might be short enough to allow continued depopulation.

These arguments are however speculative and the results of the experiments cannot at present be adequately explained on the basis of cell population kinetic principles. The experiments were designed to investigate the general predictions of a particular formula and it is not possible to determine whether the quantitative predictions of the formula are justified.

It is apparent from the results that the alternating fractionation formula in its present form is still only an approximate model of the biological reality, and it would appear that more basic information is required before it would be possible to improve the present formulation.

CHAPTER 6

A BIOLOGICAL INVESTIGATION OF THE GAP FORMULA OF
THE CRE MODEL

6.1. Introduction

A frequently recurring problem confronting the clinician in practical radiotherapy concerns the allowance that must be made for the amount of repair and of recovery from damage to the irradiated tissue which occurs when a gap in treatment is introduced, either by accident or design. Most fractionated radiotherapy is designed to produce the maximum amount of damage to the neoplastic tissue whilst sparing the surrounding normal tissue. This is very often achieved by giving that total dose, for any particular time schedule, which produces damage in the normal connective tissue at the upper level of tolerance. That is the amount of irradiation damage which the tissue can tolerate without being permanently and irretrievably injured.

Obviously a gap introduced at some stage in the schedule will allow time for recovery which has to be taken into consideration when treatment is recommenced. If the original schedule parameters of total dose and fraction interval are adhered to when treatment begins once again, the result will be a sub-tolerant level of damage, not only sparing the normal tissue but also the malignant tissue under treatment.

There are several methods of remedying this situation. For instance the schedule can be lengthened so that an increased total dose is given, or the total time can be kept the same but the individual fraction size increased. The problem then, is how to apply one

of the remedies accurately enough to produce the desired effect without incurring the danger of over- or under-irradiation of the normal tissue.

The CRE system is based on a monotonically increasing scalar assessment of biological damage in normal connective tissue, implying that a single number, the CRE, is taken to be a complete and unambiguous description of the level of biological effect generated by the radiation regardless of the way in which the damage was inflicted, working within this framework of a scalar description of biological effect, it follows that the decay in CRE during a gap in treatment must depend only on the duration of the gap and the numerical value of the CRE achieved before the gap in treatment commenced.

It is on these premises and on the fact that the simplest feasible formulation for the loss of CRE (ie repair of damage) is that of exponential decay, that the present CRE gap formula is based (Kirk et al., 1975). This formula is quite compatible with the very limited amount of clinical data available on intervals in treatment. However, as this information is mainly obtained from schedules where the gap occurs in the middle of treatment, as in Sambrook-type techniques, there is little evidence as to the accuracy of the gap formula when applied to intervals occurring either early or late in schedules.

Thus experiments were devised to test the ability

of the CRE gap formula to accurately resolve the problem of a gap occurring at any point in a schedule.

6.2. The Experiments

The Withers crypt microcolony assay technique has been shown to be a reasonably accurate assessment of gut damage at exponential levels (chapter four). That is at levels of damage greater than that in the shoulder region of a fractionated crypt survival curve. Hence a schedule format was chosen which was known to produce a significant reduction in crypt numbers.

First a control experiment was performed and duplicated, consisting of 18 fractions of 210 rads given in 6 days. Partial body 250 kV X-irradiation was used (irradiation of the abdomen alone). Three fractions per day were administered with a fraction interval of 3 hours and an 18 hour interval between each third and fourth fraction. It was imperative that during these experiments no animal deaths should occur but that a relatively low crypt count should be achieved. Using a fraction size of 210 rads these conditions were satisfied.

The results of these standard schedule experiments are presented in Figure 6.1 as a graph of numbers of surviving crypts per circumference against total dose. It can be seen that a mean crypt count of 32 surviving crypts per circumference was achieved after 18 fractions of 210 rads, a total dose of 3780 rads.

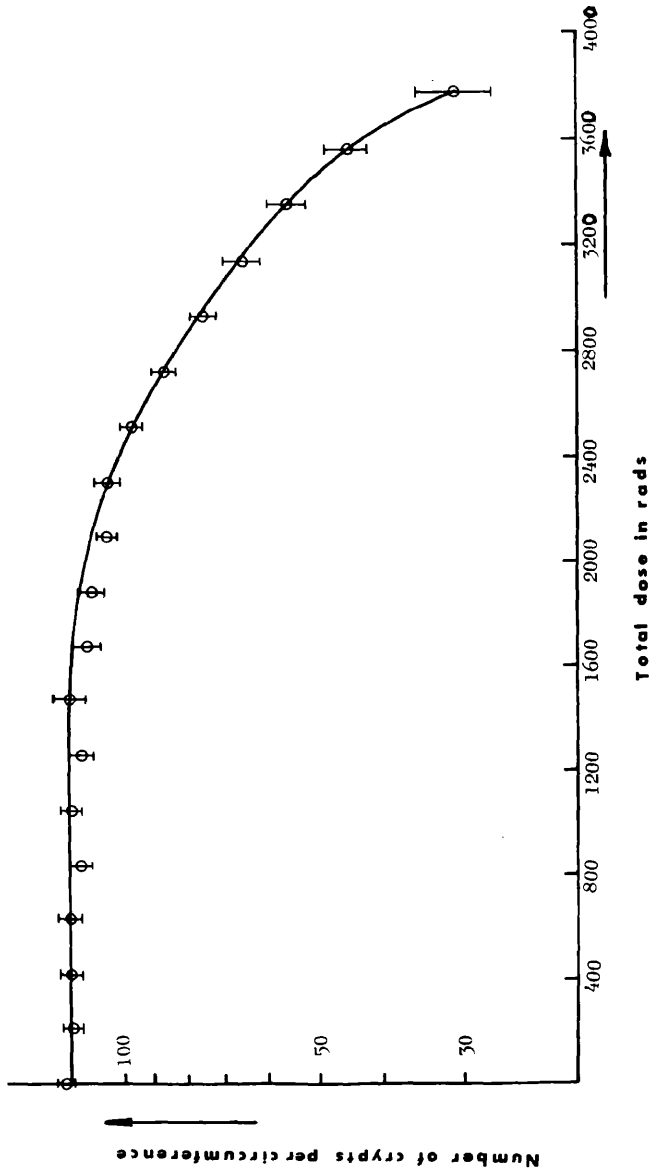


Figure 6.1
 Crypt survival curve for the standard schedule,
 (18 fractions of 210 rads of X-rays)

6.3. Gap Experiments

It was decided that during this investigation the total number of fractions, the total duration time of the schedule and the length of the gap should all be kept constant. Thus it is the position of the gap in the schedule and the size of the fractions administered after the gap which are the important factors and the only variables. The size of the gap was chosen as two days and was made to occur after each third fraction (each day), that is after 3, 6, 9, 12 or 15 fractions of 210 rads. Three or four different sized fraction doses were then chosen for the corresponding 15, 12, 9, 6 or 3 fractions following the gap, the aim being to reach as near as possible the same end-point of 32 crypts per circumference as achieved by the standard schedule. The additional dose which would achieve the necessary end-point (32 crypts) could then be determined by extrapolating lines fitted to the experimental data using an error-weighted least mean square fit.

Table III gives all the results of the gap experiments. Alongside the individual schedules are listed the additional doses per fraction after the gap and the corresponding mean counts of crypts per circumference plus the appropriate standard errors. A minimum of eight mice were used for each separate assay point in these experiments. 30 unirradiated control animals were sampled over the period of experimentation. The mean crypt count obtained from

TABLE III

<u>Schedule</u>	<u>Additional dose (rads)</u>	<u>Crypts per circumference</u>	<u>± SEM</u>
	200	82.5	2.5
<u>3 + 15</u>	220	64.9	2.3
	240	50.3	1.7
	260	31.0	3.0
	240	63.0	2.16
<u>6 + 12</u>	255	51.5	2.06
	270	37.5	2.03
	255	60.7	2.27
<u>9 + 9</u>	270	50.0	2.77
	285	38.7	3.50
	255	79.5	3.42
<u>12 + 6</u>	270	63.0	4.24
	285	50.9	3.01
	300	38.0	3.32
	220	76.0	5.01
<u>15 + 3</u>	240	55.5	2.46
	260	40.6	3.11
	280	32.4	2.39

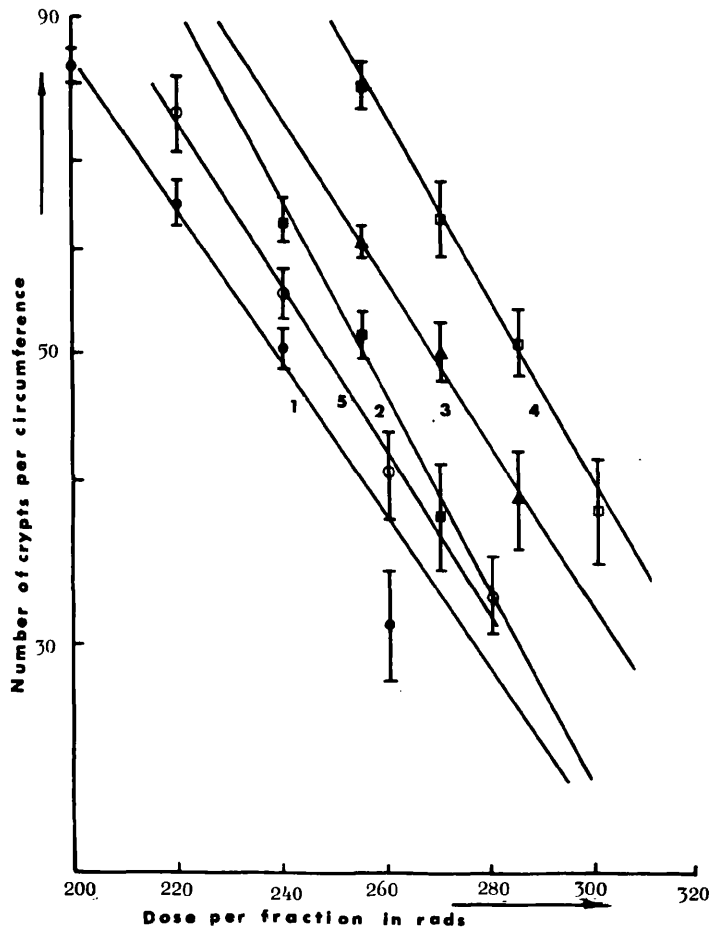
these controls was found to be $123.3 \pm$ S.E. 3.8.

The results of the gap experiments are presented in graphical form in Figure 6.2. The lines are fitted to the points of each experiment using a least mean square fit and extrapolated to a level of 32 crypts per circumference. The additional dose per fraction was then read off at this level of biological damage for each experiment. For convenience these doses along with their calculated standard errors are present in table form below the graph in Figure 6.2.

6.4. Comparison of the Results with the Predictions of the CRE Gap Formula

The experiments described were designed so that the decay in damage (or CRE) over a fixed time gap could be determined as a function of the amount of damage (CRE) which has already been achieved before the start of the gap in the schedules. This decay is measured in terms of the additional dose required in the fractions administered after the gap, to achieve a constant level of biological damage; this is characterised by the total additional dose required to achieve 32 crypts per circumference.

In Figure 6.3 the theoretical total additional dose predicted by the gap formula to compensate for the two day gaps are shown plotted against the number of fractions before the gaps (ie the position of the gaps) (from Kirk et al., 1975). If the theoretical predictions



		Fractionation schedule	Doses (rads) to give 32 crypts
1	●	3 + 15 fractions	271.4 ± 10
2	■	6 + 12 fractions	281.3 ± 9
3	△	9 + 9 fractions	299.5 ± 5
4	□	12 + 6 fractions	312.7 ± 3
5	○	15 + 3 fractions	278.7 ± 4

Figure 6.2

Graphic presentation of the results of the assay doses of the gap schedules. Table (insert) gives derived doses per fraction to give 32 crypts in each schedule.

are correct then the results of the experiments, if plotted in the same manner, should give a curve of the same shape. Figure 6.4 shows a graph of the experimental results plotted in just such a way. Comparison of Figures 6.3 and 6.4 shows that there are considerable differences between the observed results and the theoretical predictions.

Compared with the simple exponential decay of damage, as assumed in the formula, the results of the experiments demonstrate that there is a greater regeneration potential early in the schedule than predicted and a much smaller regeneration potential later in the schedule. The results suggest that as the total dose increased there is an increase in the damage to the repair capacity of the tissue, whereas the repair and repopulation potential is relatively unimpaired by a few low dose fractions (a low total dose).

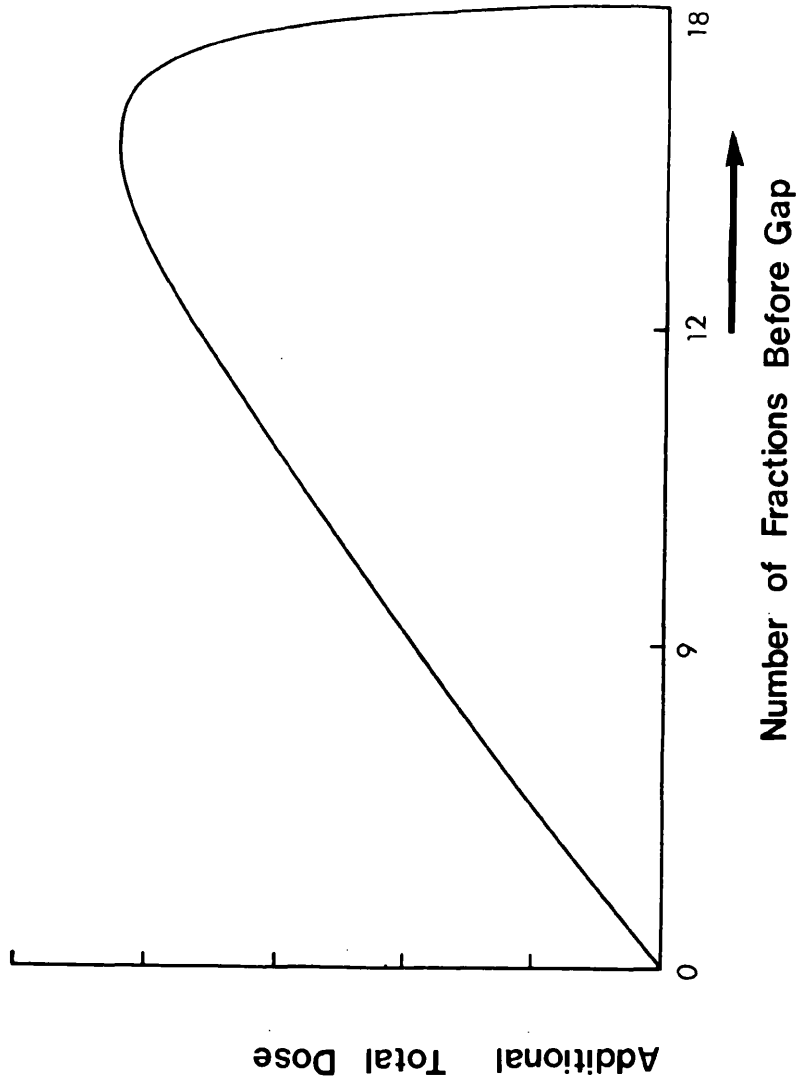


Figure 6.3
 Theoretical total dose required to achieve the same end point (amount of damage) plotted as a function of the position of the gap.

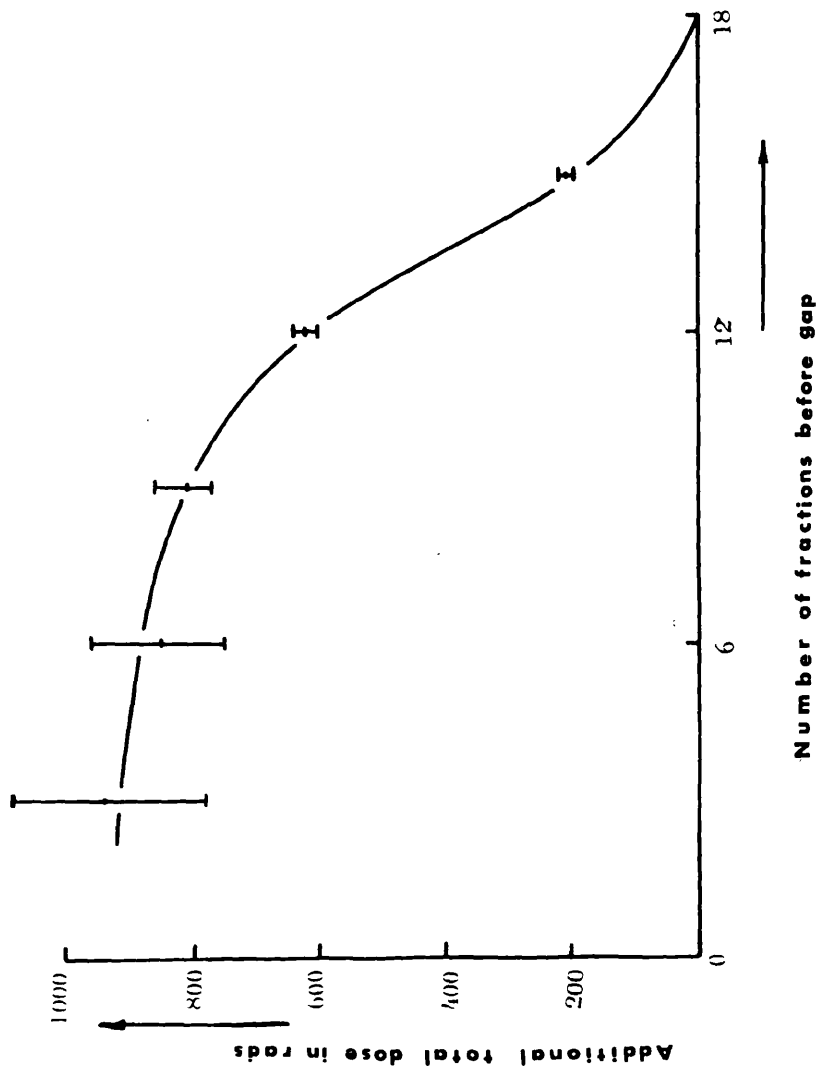


Figure 6.4

Experimental results presented in same format as figure 6.3 for easy comparison of actual and predicted results.

6.5. Discussion and Conclusions

Cell repopulation in the mouse intestinal crypt system achieves essentially a maximum regeneration rate within a very short time after a dose of radiation. So although this might not be the only reason, it is possible that a high additional dose after a gap early in treatment might be required, to reach the desired level of damage, with gut tissue. This may not necessarily be the case in other tissues (eg skin) for which the CRE model was originally designed.

In a tissue such as normal skin it is known that the repair potential is increased in response to damage up to a maximum level. A series of experiments to determine the amount of repair in skin tissue during an interval in treatment has been reported by Denekamp (1973). In these experiments, mouse feet were irradiated with either four, nine or 30 fractions of 300 rads in five daily fractions. Single doses were given immediately following the last fraction or after one, three, seven or 14 days to achieve a chosen end-point. It has been demonstrated (Perry, Hamlet and Kirk, 1979) that Denekamp's results when subject to an analysis using CRE parameters show that a lower additional dose is required earlier in treatment than has been found to be required with the results of the mouse gut experiments described in this chapter. The results of the gut experiments have demonstrated, as noted earlier, that repair potential decreases with

increasing total dose and that at higher dose levels there is no longer an exponential decay of damage during the gap in treatment.

As an hypothesis the above observations may be summarised in the form shown diagrammatically in Figure 6.5, where the regeneration potential is plotted against the level of biological effect achieved before a gap occurs. Thus, for a tissue such as skin the regeneration potential rises to a maximum in response to a small amount of damage and then falls asymptotically as the radiation damage approaches tolerance.

Several biological mechanisms must be involved in such a response. After a radiation insult, a cell population increases its rate of repopulation but under conditions of increasing levels of damage the population becomes increasingly incapable of repair, thus leading to a turning point and fall in the regeneration potential.

Recent publications (Brown and Probert, 1975; Hendry et al., 1977; and Hunter and Stewart, 1977) indicate that some time after a near-tolerance treatment schedule, almost as much radiation can again be given although some memory of the previous damage clearly exists. The amount of re-irradiation which can be tolerated appears to depend upon the target tissue. Therefore, although the initial decay in effect following treatment may be fairly rapid, residual damage cannot be neglected as an important aspect of tissue regeneration after treatment.

In conclusion it can be said that existing methods

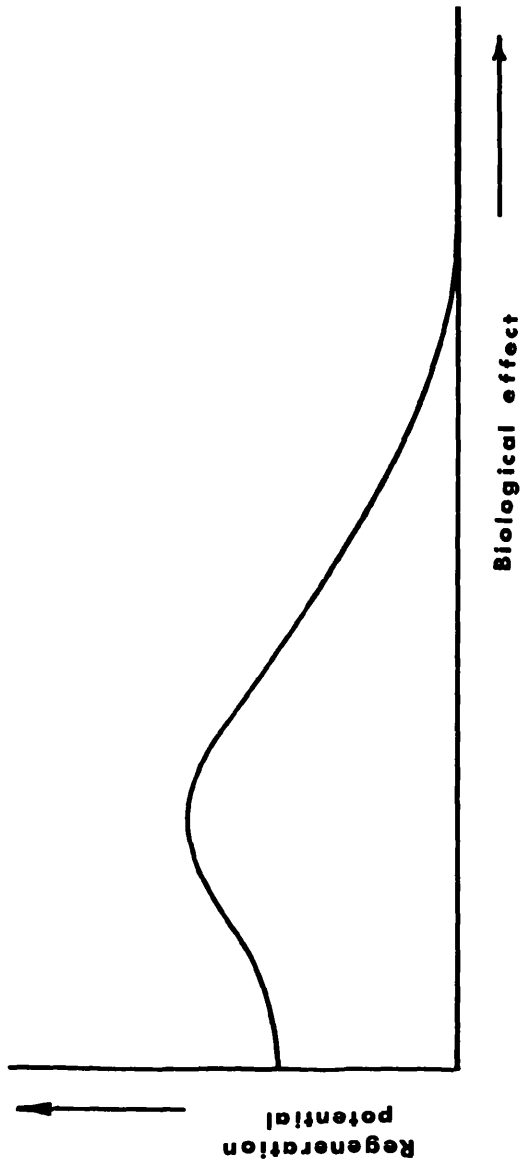


Figure 6.5
Hypothetical representation of how regeneration potential varies
with increasing total dose.

of allowing for intervals in treatment are inadequate. From the presently available evidence it appears that there are at least three biological concepts which must be taken into consideration if a more realistic biological description is to be formulated.

1. Increasing regeneration potential early in treatment in certain tissues.
2. Progressive loss of regenerative potential with increasing damage.
3. Longer term residual level of biological effect.

The mouse gut experiments were not aimed at offering a solution to the problems concerning gaps in treatment but to test the limitations of the CRE gap formula in its current form. There is sufficient evidence to suggest a need to rethink the formulation before it is adequate to the needs of the clinical practitioner in radiotherapy. However, the formulation can not be restructured without much more biological evidence than is presently available. So there is an accompanying vital need for more experimental data relevant to the problem.

CHAPTER 7

SUMMARY OF CONCLUSIONS AND DISCUSSION OF SOME
POSSIBLE FUTURE DEVELOPMENTS

7.1. Introduction

This chapter presents an examination of the more salient conclusions which were reached in the discussions of the previous chapters. It is an attempt to try and assess the relevant significance of these conclusions with reference to the practice of modern radiotherapy. The discussion will however, also refer to possibilities which may have been disclosed by various aspects of the work presented, that might previously not have been widely recognised or accepted.

This section is then followed by a brief survey of some of the fields in which further investigation might prove to be profitable.

7.2. Surface Morphology after Single Doses of Neutron Irradiation

The data presented in chapter three led to the drawing of the conclusion that for whatever reasons neutron irradiation produces its own distinctive pattern of damage in the gut. This pattern was seen as a much more marked tendency towards flattened and conical villi than is seen after gamma irradiation, where the villi generally retain their initial slender contours. Also neutron irradiation produced a marked change in surface creasing and it was noted that the banding and twisting of villi seen after gamma irradiation is usually absent after neutron irradiation.

It is possible to speculate that this pattern of

damage is not wholly attributable to the damage caused in the epithelial cell population but may also be concerned with injury to the underlying connective and vascular tissue. From the standpoint of clinical radiotherapy it is important that the reasons for the production of this pattern of damage are investigated, as neutron therapy is a treatment modality in use in some centres at the present time and is likely to become more common in the future.

7.3. Surface Morphology after Fractionated Doses of X and Gamma Irradiation

The discrepancies found between the observations made with conventional histological techniques and scanning electron microscopy after fractionated doses of X and gamma irradiation (as described in chapter four) are worthy of special consideration. It was expected that a fractionation schedule extending over a period of time much in excess of the transit time of the intestinal cell population from crypt to villus tip would effect a situation whereby the extent of crypt damage would be reflected in the amount of villus damage and vice versa. This expectation was confirmed by the data from one of the experimental treatment schedules (Schedule C. 250 rads X-irradiation given three times per day), but not by the data obtained from a second schedule (Schedule A. Daily fraction of 300 rads gamma irradiation plus a 900 rad assay dose) and only to a

small extent by a third schedule (Schedule B. Daily fractions of 450 rads gamma irradiation).

Previous publications have expressed the opinion that under continuous radiation the intestine (in the rat) would maintain function almost indefinitely (Lamerton and Lord, 1964). Masuda and co-workers (1977) have put forward the view, based on data obtained with the microcolony technique, that present information derived from mouse studies would allow the treatment of volumes including the intestine to be carried out with some safety. The results of the experiments from Schedule A, which is in fact a schedule very similar to one in use clinically, demonstrate that high levels of surviving cells in the crypts of Lieberkuhn do not always correlate with low levels of damage to the gut mucosa.

These observations lead to the conclusion that if the conditions found in the mouse can be extrapolated to the human situation, an unexpectedly high level of damage might be produced in the surface mucosa. This might in turn lead to undesirable consequences. Thus radiation treatment involving any of the intestinal tract using an equivalent regime of Schedule A should only be carried out with extreme caution.

- 7.4. The Alternating Fractionation Formula of the C.R.E. Model
- The experimental results described in chapter five have demonstrated that this formula has certain limitations.

Whilst it correctly predicts an increased effect with alternating fractionation as against a standard schedule, it is in error in predicting that the order in which alternate fractions are administered will not affect the total amount of biological damage that is produced.

It will be remembered that the schedules in which each individual fraction was alternated produced a greater effect than those schedules where all the low dose fractions were given before all the high dose fractions (or vice versa).

However, there is at the present time, insufficient data to suggest that the formula should be withdrawn from clinical use. It is certainly only an approximation of the biological reality, but as a tool for use in clinical practice this formula is possibly one of the best approximations currently available.

7.5. The Gap Formula of the C.R.E. Model

The results obtained from the experiments described in chapter six, which were designed to investigate the gap formula, demonstrate that in its present form, the formula has several defects. Principally the formula predicts erroneous effects after a gap which occurs either early or late in a treatment schedule.

Basically the formula at present assumes that during a gap in treatment recovery proceeds at an exponential rate, and that this exponential decay rate of damage is

constant and not dependent on the position of the gap in the treatment schedule. However, the experiments have shown that in the mouse gut, a much greater amount of recovery occurs during a gap which occurs early in treatment, than is predicted by the formula. The results also demonstrate that during a gap which occurs late in treatment there is a much smaller amount of recovery than that predicted by the formula. Thus the rate of decay of damage during a gap in treatment is dependent on just where the gap occurs (i.e. its position in the treatment schedule). In other words the regeneration potential of the tissue is dependant on the amount of damage accumulated.

Therefore it can be concluded that the CRE gap formula does not adequately allow for intervals in treatment, and that any new formulation based on the present model must also take into account the following properties of tissue.

1. An increased regeneration potential early in treatment.
2. Progressive loss of regeneration potential as the level of damage increases.
3. Longer term residual damage.

In fact, the mathematicians responsible for the original derivation of the gap formula are at present engaged in an attempt to formulate a more realistic mathematical model based on these conclusions.

FURTHER WORK

7.6. Experiments Commenced

The investigations involving Scanning electron microscopy produced some observations requiring further clarification. It is possible that the pattern of neutron damage observed in the experiments in chapter three and the scanning observations made after fractionated irradiation (chapter four) might have shown other variations if a different time of assay had been chosen.

To investigate these possibilities a set of experimental procedures was instigated. Unfortunately, due to the lack of available time on the irradiation facilities these experiments have not been completed at this time. Therefore it is not possible to comment on what effect the time of assay has on scanning observations after fractionated schedules. However, there is data presently available which indicates that the neutron damage pattern is consistent up to a time $5\frac{1}{2}$ days after irradiation.

Briefly, mice were irradiated with single doses of 900 rads of X or gamma irradiation or alternatively 500 rads of neutron irradiation and then killed at $\frac{1}{2}$ day intervals after irradiation. No damage consistent with the neutron pattern occurs after gamma or X-irradiation from $\frac{1}{2}$ to $5\frac{1}{2}$ days after irradiation. Also no damage consistent with the gamma pattern is found after neutron irradiation over the same time scale. These results

strongly support the conclusion that neutron irradiation produces, for whatever reasons, its own distinctive pattern of damage in the surface mucosa of mouse gut.

7.7. Some Possible Future Developments

It has been noted previously (chapter three) that it is possible that the patterns of radiation damage in the intestinal villi are not primarily due to the damage in the epithelial cell population but may be concerned with the damage to the underlying connective and vascular tissue. Different approaches are available to investigate these possibilities. Several different stains are available which would allow histological preparations to be examined microscopically for changes in the gut vasculature. A technique is now available which allows the removal of the surface epithelium of the villi whilst leaving the stroma intact. The specimens of intestine are simply left in normal (physiological) saline for four days, opened longitudinally and washed. This removes the epithelial layer and after appropriate fixation and coating, scanning microscopical examination can be carried out. This technique might be useful for the examination of the connective tissue in gut villi for signs of irradiation damage.

Further investigations might also be carried out with the scanning electron microscope, into the effect

of other fractionation schedules on the villi of the intestine. Of particular interest would be an investigation using fractionated schedules involving neutron irradiation, either on its own or in conjunction with gamma or X-irradiation.

The investigations of the Alternating fractionation and Gap formulae of the CRE model have shown that considerably more work is necessary to expedite the process of modification of the formulae to achieve more realistic models. It is possible that a different biological model might prove more valuable for further provision of experimental data. Experiments are already planned, using the mouse tail skin assay technique of Hendry and co-workers (Hendry et al., 1976) to investigate the biological concepts underlying the theory behind the gap formula. If successful it is hoped that these attempts will lead to an improved formula for use in clinical practice.

Mouse skin and gut might also be used as biological models for testing predictive formula concerned with neutron irradiation, as it is at present possible to see a clinical application for such formulae in neutron therapy.

APPENDICES

APPENDIX 1

Experimental X-irradiation Facility

During a period of re-equipment a Siemens Stabilipan I X-ray unit became available for use as an experimental irradiation source. As space and finance to provide and equip the usual well shielded room were not available, a solution was sought which resulted in the construction of the shielding unit described in this appendix.

Accommodation for the machine, shielding unit and ancillary equipment was made available by the conversion of an infrequently used store room. Water, drainage and electricity supplies were installed by hospital engineers, but installation of the X-ray machine was carried out by representatives of Siemens Ltd.

The construction of the shielded box is shown schematically in Fig. A1. It consists of lead ply supported on a simple metal frame. A collimator limited the beam area so that only the top surface of the box was in the direct beam. This surface was shielded with an additional 5 mm of lead. An interlock prevented the X-ray beam being switched on whilst the door of the box was open. The door was hinged along the bottom edge, so that when open and supported by a strong safety chain, it formed a useful shelf. Materials for irradiation were placed on a perspex shelf, the height of which is adjustable. The central-axis surface dose rates at the highest and lowest positions are 24 and 136 rad minute⁻¹ respectively.

Safety checks on radiation levels from the unit were carried out by the area Radiological Protection Adviser. Measurements were made of the exposure rate through the lead

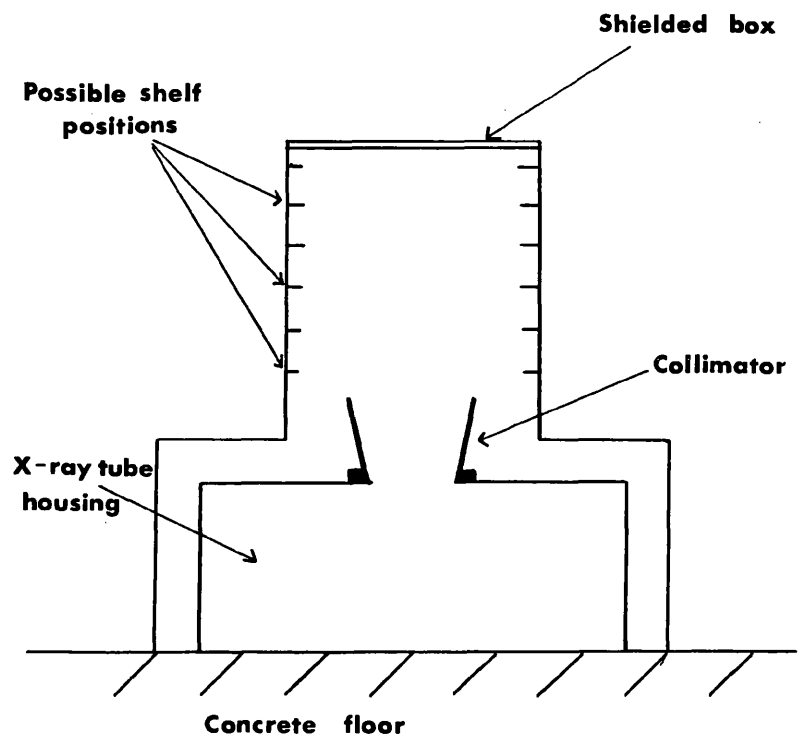


Diagram of shielding unit.

when the tube was operating at its maximum output. These were made with an ionisation chamber both in contact with the box and also approximately one metre from the tube focus. The maximum values obtained were 30 milli-Roentgen per hour and 2.5 milli-Roentgen per hour respectively. These levels are well within the allowed limits set down in the Code of Practice. The Radiological Protection Adviser also made recommendations on the use of the machine and on various factors effecting the safety of the operators and other personnel. Principally these require that all persons remain at least one metre from the box while the tube is in operation, and that the total running time of the equipment be limited to 20 hours per week.

Fundamentally the unit was constructed so as to provide facilities for whole and partial body irradiations of small animals at a reasonably wide range of dose rates and using X-rays of sufficient hardness to deliver a homogeneous dose distribution throughout the tissues of these experimental animals. However it has also been used for irradiating cells in tissue culture contained in a variety of plates, tubes and bottles.

APPENDIX II

During the course of the investigations reported in this thesis it was sometimes necessary to perform experiments to clear up small points or answer possible criticisms of the conclusions drawn from the data obtained. These experiments, although important, are ancillary to the main body of work and if reported earlier would have disturbed the flow of the descriptive chapters. Hence they are briefly described in this appendix.

Split Dose Experiments

In chapter four the first fractionation schedule (A) had a daily fraction dose of 300 rads plus an 'assay' dose of 900 rads of ^{60}Co Cobalt gamma irradiation. This assay dose was used in the hope of reducing crypt cellularity so that damage could be assayed on that portion of the crypt survival curve which shows some structure. It is obvious from the results that it failed in this function. Split dose experiments were performed using 900 rads gamma as a first dose. The data are presented in Figure A2. It is clear that the 'shoulder' of the crypt survival curve is 'reconstructed' so that the total dose is approximately 450 rads greater than that of the single dose curve, for the same level of damage. In other words the D_2-D_1 value is 450 rads. This observation confirms the findings of other workers (Withers et al., 1970; Hendry and Potten, 1974). Thus because of the recovery from sub-lethal damage and rapid repopulation of the crypts even a relatively large dose of 900 rads has a relatively small effect on crypt

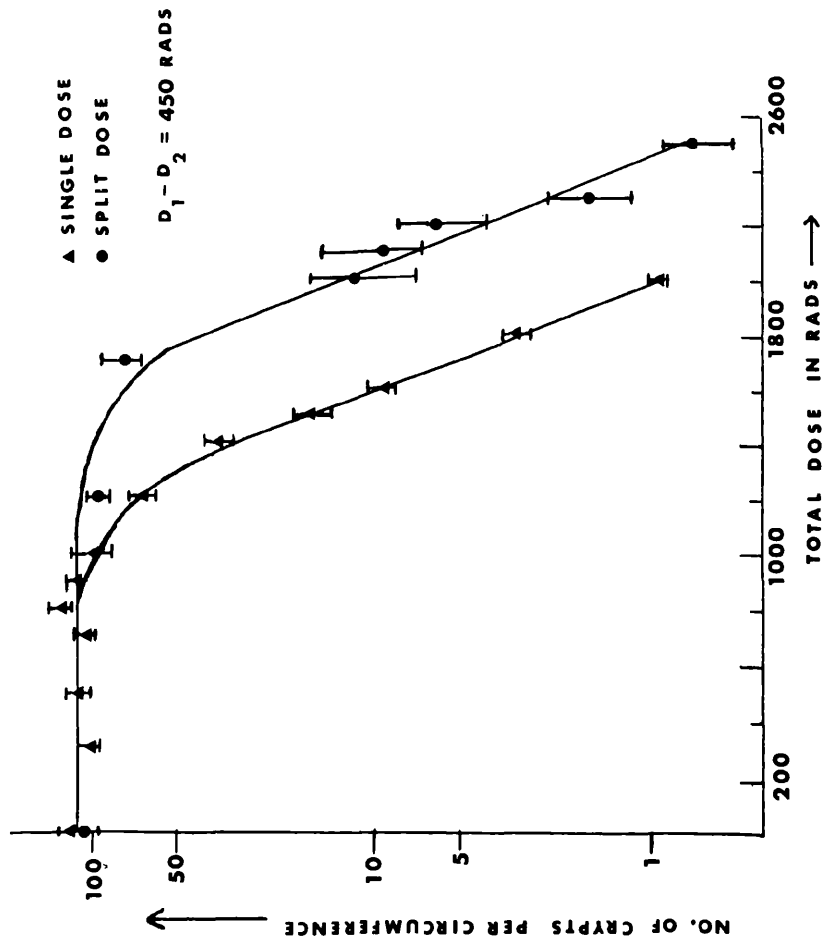


Figure A2

Results of Split dose Experiments. First dose 900 rads;
 Time interval between doses 24 hours.

numbers. If however, in Schedule A (Chapter 4), a larger dose had been used, or the same dose been given at a shorter time interval the probable result would have been an increase in the number of deaths from bone marrow failure and hence the object of the assay dose would have been further frustrated.

Whole and Partial Body Irradiation

At the start of the projects the sources of irradiation available were a D-T neutron generator and a ⁶⁰Cobalt gamma therapy machine. Because of difficulties with shielding it was possible to carry out only whole body irradiation using these facilities. Sometime later however an X-irradiation machine became available for experimental work (as described in Appendix I) and this allowed partial body irradiations to be performed.

Experiments were designed to investigate the differences of gut (crypt) response due to RBE effects and differences due to the use of whole body gamma or partial body (to the abdomen alone) X-irradiation. Surprisingly perhaps, these experiments showed that there is no significant difference in crypt counts after single whole body doses of gamma irradiation and single partial body doses of 250 kV X-irradiation.

There is undoubtedly an RBE effect (Sigdestad et al., 1972; Greene et al., 1975), but this is small and difficult to detect accurately with the crypt counting system. In further experiments using whole body gamma and whole body X-irradiation an RBE of 0.9 was obtained for gamma irradiation

as compared to X-irradiation. However, it has been demonstrated that crypt numbers and intestinal cell kinetics in general show significantly different degrees of effect after localised as opposed to whole body irradiation, (Leshner and Bauman, 1969; Leshner and Leshner, 1974; and Hamilton, 1977) in that whole body irradiation is generally more effective. It can only be conjectured therefore, that the increased effect produced by whole body gamma irradiation has counterbalanced the larger RBE of partial body X-irradiation. That is in these two specific conditions of irradiation the opposing effects have cancelled each other out. This allows then, direct comparisons to be made (with particular relevance to the work described in Chapter 4) between results obtained from animals subjected to either whole body gamma or partial body X-irradiation.

Partial Body Irradiation (Irradiation Technique)

The possibility existed that practical deficiencies of the partial body irradiation procedure might influence the results of fractionation experiments using this type of irradiation. It could have been that the positioning of the animals had varied from exposure to exposure. To test this mice were irradiated with single doses of 1000 or 1400 rads of X-rays and fractionated doses of 2730 or 2950 rads given in 13 or 15 fractions using the same irradiation procedure. The animals were left until the characteristic post-irradiation unpigmented hair appeared (see Fig. A3). This was found to occur in a sharply defined band involving the whole of the

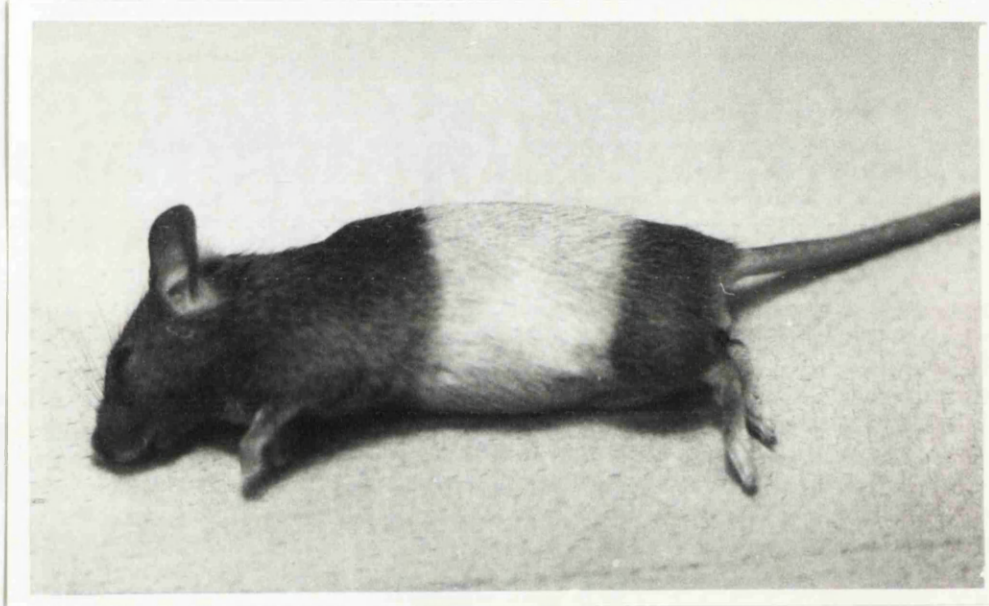


Figure A3

Photograph of mouse showing classic post-irradiation pigment loss in the irradiated area.

area around the abdominal cavity. This provides final confirmation that all of the abdominal cavity and thus all of the gastro-intestinal tract was in the irradiation field during exposure.

Conclusions

All of the experiments described in this appendix have proved to have had a bearing on the investigations described in the previous chapters and in some cases to have helped in the understanding of the results obtained.

REFERENCES

CHAPTER 1

- WITHERS, H.R. and ELKIND, H.M., 1970. Microcolony survival assay for cells of mouse intestinal mucosa exposed to radiation. *Internal Journal of Radiation Biology*. 17, 261.
- ELLIS, F., 1968. The relationship of biological effect to dose-time-fractionation factors in radiotherapy. In *Current Topics of Radiation Research*, Ed. M. Ebert and A. Howard, Vol. 4. Amsterdam: North-Holland Publ. Co. pp. 357-397.
- ORTON, C.G. and ELLIS, F., 1973. A simplification in the use of the NSD concept in practical radiotherapy. *British Journal of Radiology*. 46, 529.
- KIRK, J., GRAY, W.H. and WATSON, E.R., 1971. Cumulative radiation effect. Part I: Fractionated treatment regimes. *Clinical Radiology*. 22, 145.
- LEBLOND, C.P. and WALKER, B.F., 1956. Renewal of cell populations. *Physiology Review*. 36, 255.
- QUASTLER, H. and HAMPTON, J.C., 1962. Effects of ionizing radiation on the fine structure and function of intestinal epithelium of the mouse. 1. Villus epithelium. *Radiation Research*. 17, 914.
- QUASTLER, H. and SHERMAN, F.G., 1959. Cell population kinetics in the intestinal epithelium of the mouse. *Experimental Cell Research*. 17, 420.
- SHERMAN, F.G. and QUASTLER, H., 1960. DNA synthesis in irradiated intestinal epithelium. *Experimental Cell Research*. 19, 343.
- FRY, R.J.M., LESHER, S. and KOHN, H.I., 1961. Age effect on cell transit time in mouse jejunal epithelium. *American Journal of Physiology*. 201, 213.
- LESHER, S., FRY, R.J.M. and KOHN, H.I., 1961. Age and the generation time of the mouse duodenal epithelial cell. *Experimental Cell Research*. 24, 334.
- LIPKIN, M. and QUASTLER, H., 1962. Cell population kinetics in the colon of the mouse. *Journal of Clinical Investigations*. 41, 141.
- LEBLOND, C.P. and STEVENS, C.E., 1948. The constant renewal of the intestinal epithelium in the albino rat. *Anat. Rec.* 100, 357.
- BERTALANFY, F.D. and LAU, C., 1962. Cell renewal. *International Review of Cytology*. 13, 359.
- LESHER, S., FRY, R.J.M. and KOHN, H.I., 1961. Influence of age on transit time of cells of mouse intestinal epithelium. I.

Duodenum. Laboratory Investigation. 10, 291.

FRY, R.J.M., LESHER, S. and KOHN, H.I., 1962. Influence of age on the transit time of cells of the mouse intestinal epithelium. III. Ileum. Laboratory Investigation. 11, 289.

LIPKIN, M., SHERLOCK, P. and BELL, B., 1963. Cell proliferation kinetics in the gastrointestinal tract of man. II. Cell renewal in Stomach, Ileum, Colon and Rectum. Gastroenterology. 45, 721.

WITHERS, H.R., BRENNAN, J.T. and ELKIND, M.M., 1970. The response of stem cells of intestinal mucosa to irradiation with 14 MeV neutrons. British Journal of Radiology. 43, 796.

HORNSEY, S., 1970. Differences in survival of jejunal crypt cells after radiation delivered at different dose rates. British Journal of Radiology. 43, 802.

WITHERS, H.R., CHU, A.M., REID, B.O. and HUSSEY, D.H., 1975. Response of Mouse Jejunum to multifraction radiation. International Journal of Radiation Oncology, Biology and Physics. 1, 41.

WITHERS, H.R., MASON, K., REID, B.O., DUBRAVSKY, N., BARKLEY, H.T., BROWN, B.W. and SMATHERS, J.B., 1974. Response of mouse intestine to neutrons and gamma rays in relation to dose fractionation and division cycle. Cancer. 34, 39.

HENDRY, J.H., MAJOR, D. and GREENE, D., 1975. Daily D-T neutron irradiation of mouse intestine. Radiation Research. 63, 149.

CHEN, K.Y. and WITHERS, H.R., 1972. Survival characteristics of stem cells of gastric mucosa in C₃H mice subjected to localized gamma irradiation. International Journal of Radiation Biology. 21, 521.

HAGEMANN, R.F., SIGDESTAD, C.P. and LESHER, S., 1970. A method for quantitation of proliferative intestinal mucosal cells on a weight basis: Some values for C57 Bl/6. Cell Tissue Kinetics. 3, 21.

WIMBER, D.E., QUASTLER, H., STEIN, O.L. and WIMBER, D.R., 1960. Analysis of tritium incorporation into individual cells by autoradiography of squash preparations. Journal of Biophysics, Biochemistry and Cytology. 8, 327.

HAGEMANN, R.F., SIGDESTAD, C.P. and LESHER, S., 1971. Intestinal crypt survival and total and per crypt levels of proliferative cellularity following irradiation: Single X-ray exposures. Radiation Research. 46, 533.

HAGEMANN, R.F., SIGDESTAD, C.P. and LESHER, S., 1971. Intestinal crypt survival and total and per crypt levels of

proliferative cellularity following irradiation: Fractionated X-ray exposures. Radiation Research. 47, 149.

SIGDESTAD, C.P., HAGEMANN, R.F. and SCOTT, R.M., 1973. The effects of oxygen on intestinal crypt survival in Cobalt-60-irradiated mice. Radiation Research. 54, 102.

SIGDESTAD, C.P., SCOTT, R.M., HAGEMANN, R.F. and DARDEN, E.B., 1972. Intestinal crypt survival: The effect of Cobalt-60, 250 kVcp X-rays and fission neutrons. Radiation Research. 52, 168.

HAGEMANN, R.F., 1976. Intestinal cell proliferation during fractionated abdominal irradiation. British Journal of Radiology. 49, 56.

RUBIN, C.E., BRANDBORG, L.L., PHELPS, F.C. and TAYLOR, H.C., 1960. The apparent identical and specific nature of the duodenal and proximal jejunal lesion in coeliac disease and idiopathic steatorrhea. Gastroenterology. 38, 28.

HOLMES, R., HOURIHANE, D. O'B. and BOOTH, C.C., 1961a. Dissecting microscope appearances of jejunal biopsy specimens from patients with idiopathic steatorrhea. Lancet. 1, 81.

HOLMES, R., HOURIHANE, D. O'B. and BOOTH, C.C., 1961b. The mucosa of the small intestine. Post-graduate Medical Journal. 37, 717.

MARSH, M.N., SWIFT, J.A. and WILLIAMS, E.D., 1968. Studies of small intestinal mucosa with the scanning electron microscope. British Medical Journal. 4, 95.

JACQUES, W.E., COALSON, J. and ZERVINS, A., 1965. Application of the scanning electron microscope to human tissues. A preliminary study. Experimental and Molecular Pathology. 4, 576.

MARSH, M.N. and SWIFT, J.A., 1969. A study of the small intestinal mucosa using the scanning electron microscope. Gut. 10, 940.

TONER, P.G. and CARR, K.E., 1969. The use of scanning electron microscopy in the study of the intestinal villi. Journal of Pathology and Bacteriology. 97, 611.

CARR, K.E. and TONER, P.G., 1972. Surface studies of acute radiation injury in the mouse intestine. Virchows Arch. Abt. B. Zellpath. 11, 201.

ANDERSON, J.H. and WITHERS, H.R., 1973. Scanning electron microscope studies of irradiated rat intestinal mucosa. In Scanning Electron Microscopy, Proceedings of the Workshop on Scanning Electron Microscopy in Pathology. IIT Research Institute, Chicago, Illinois. Pages 565 to 572.

ELLIS, F., 1967. Fractionation in Radiotherapy. Deeley, T.J. and WOOD, C.A.P. (eds.): Modern Trends in Radiotherapy. Vol. I, Ch. II, pp. 34-51. Butterworths, London.

ELLIS, F., 1969. Dose, time and fractionation: A clinical hypothesis. Clinical Radiology. 20, 1.

WINSTON, B.M., ELLIS, F. and HALL, E.J., 1969. The Oxford NSD calculator for clinical use. Clinical Radiology. 20, 8.

COHEN, L., 1960. Ph.D. Thesis, University of Witwatersrand.

KIRK, J., GRAY, W.M. and WATSON, E.R., 1972. Cumulative radiation effect. Part II: Continuous radiation therapy - long lived sources. Clinical Radiology. 23, 93.

KIRK, J., GRAY, W.M. and WATSON, E.R., 1973. Cumulative radiation effect. Part III: Continuous radiation therapy - short lived sources. Clinical Radiology. 24, 1.

KIRK, J., GRAY, W.M. and WATSON, E.R., 1975. Cumulative radiation effect. Part V: Time gaps in treatment regimes. Clinical Radiology. 26, 159.

CHAPTER 2

LAWSON, R.C., PORTER, D. and HANNAN, W.J., 1972. Threshold detector measurements with sealed tube D-T neutron generators. Physics in Medicine and Biology. 17, 771.

GREENIE, D., 1971. An ionization chamber for the dosimetry of 14 MeV neutron beams. Physics in Medicine and Biology. 16, 489.

BEMLEY, D.K., McCULLOUGH, E.C., PAGE, B.C. and SAKATA, S., 1972. Determination of absorbed dose in a fast neutron beam by ionization and calorimetric methods. Proceedings of First Symposium on Neutron Dosimetry.

CHAPTER 3

WITHERS, H.R. and ELKIND, M.M., 1970. Microcolony survival assay for cells of mouse intestinal mucosa exposed to radiation. International Journal of Radiation Biology. 17, 261.

WITHERS, H.R., BRENNAN, J.T. and ELKIND, M.M., 1970. The response of stem cells of intestinal mucosa to irradiation with 14 MeV neutrons. British Journal of Radiology. 43, 796.

HAGEMANN, R.F., SIGDESTAD, C.P. and LESHER, S., 1970. Quantitation of intestinal villus cells on a weight basis: values for C57 BL/6 mice. American Journal of Pathology. 218, 637.

HAGEMANN, R.F., SIGDESTAD, C.P. and LESHER, S., 1971. Intestinal crypt survival and total per crypt levels of proliferative cellularity following irradiation: Single X-ray exposures. *Radiation Research*. 46, 533.

LESHER, S., 1967. Compensatory reactions in intestinal crypt cells after 300 roentgens of cobalt-60 gamma irradiation. *Radiation Research*. 32, 510.

CARR, K.E. and TONER, P.G., 1968. Scanning electron microscopy of rat intestinal villi. *Lancet*. 2, 570.

TONER, P.G. and CARR, K.E., 1969. The use of scanning electron microscopy in the study of the intestinal villi. *Journal of Pathology and Bacteriology*. 97, 611.

BROERSE, J.J., BARENDSEN, G.W., FRERIKS, G. and VAN PUTTEN, L.M., 1971. RBE values of 15 MeV neutrons for effects on normal tissues. *European Journal of Cancer*. 7, 171.

ANDERSON, J.H. and WITHERS, H.R., 1973. Scanning electron microscope studies of irradiated rat intestinal mucosa. In *Scanning Electron Microscopy, Proceedings of the Workshop on Scanning Electron Microscopy in Pathology*. IIT Research Institute, Chicago, Illinois.

CHAPTER 4

HAMLET, R., CARR, K.E., TONER, P.G. and NIAS, A.H.W., 1976. Scanning electron microscopy of mouse intestinal mucosa after cobalt 60 and D-T neutron irradiation. *British Journal of Radiology*. 49, 624.

HENDRY, J.M. and POTTEN, C.S., 1974. Cryptogenic cells and proliferative cells in intestinal epithelium. *International Journal of Radiation Biology*. 25, 583.

ANDERSON, J.H. and WITHERS, H.R., 1973. Scanning electron microscope studies of irradiated rat intestinal mucosa. *Scanning Electron Microscopy. Proceedings of the Workshop on Scanning Electron Microscopy in Pathology*.

CARR, K.E. and TONER, P.G., 1972. Surface studies of acute radiation injury in the mouse intestine. *Virchows Arch. Abt. B. Zellpath.* 11, 201.

JACKSON, K.L., RHODES, R. and ENTENMAN, C., 1958. Electrolyte excretion in the rat after severe intestinal damage by X-irradiation. *Radiation Research*. 8, 361.

CURRAN, P.F., WEBSTER, E.W. and HORVEPIAN, J.A., 1960. The effect of X-irradiation on sodium and water transport in rat ileum. *Radiation Research*. 13, 369.

HAGEMANN, R.F. and CONCANNON, J.P., 1975. Time/dose relationships in abdominal irradiation: a definition of principals and experimental evaluation. *British Journal of Radiology*. 48, 545.

HAGEMANN, R.F., 1976. Intestinal cell proliferation during fractionated abdominal irradiation. *British Journal of Radiology*. 49, 56.

WITHERS, H.R., CHU, A.H., REID, B.O. and HUSSEY, D.H., 1975. Response of mouse jejunum to multifraction radiation. *International Journal of Radiation Oncology, Biology and Physics*. 1, 41.

WAMBERSIE, A., DUPREIX, J., GUEULETTE, J. and LELLOUGH, J., 1974. Early recovery for intestinal stem cells, as a function of dose per fraction, evaluated by survival rate after fractionated irradiation of the abdomen of mice. *Radiation Research*. 58, 498.

ROSWIT, B., MALSKY, S.J. and REID, C.P., 1972. Severe radiation injuries of the stomach, small intestine, colon and rectum. *American Journal of Roentgenology*. 114, 460.

WELLWOOD, J.M. and JACKSON, B.T., 1973. The intestinal complications of radiotherapy. *British Journal of Surgery*. 60, 814.

CHAPTER 5

KIRK, J., 1975. Cumulative radiation effect: some qualitative predictions. *Proceedings of the 6th L.H. Gray Conference*. Ed. T. Alper. (Pub. Institute of Physics and John Wiley and Sons Ltd.) pp. 320-327.

KIRK, J., GRAY, W.M. and WATSON, E.R., 1971. Cumulative radiation effect. Part I: Fractionated treatment regimes. *Clinical Radiology*. 22, 145.

CHAPTER 6

KIRK, J., GRAY, W.M. and WATSON, E.R., 1975. Cumulative radiation effect. Part V: Time gaps in treatment regimes. *Clinical Radiology*. 26, 159.

DENEKAMP, J., 1973. Changes in the rate of repopulation during multifraction irradiation of mouse skin. *British Journal of Radiology*. 46, 381.

PERRY, A.M., HALLET, R. and KIRK, J., 1979. Investigation of time-gap formulae on the CRE system using mouse tissue as a biological model. *British Journal of Cancer*. 40, 649.

BROWN, J.M. and PROBERT, J.C., 1975. Early and late radiation changes following a second course of irradiation. *Radiology*. 115, 711.

HENDRY, J.H., ROSENBERG, I., GREENE, D. and STEWART, J.G., 1977. Re-irradiation of rat tails to necrosis at six months after treatment with a "Tolerance" dose of X-rays or neutrons. *British Journal of Radiology*. 50, 567.

HUNTER, R.D. and STEWART, J.G., 1977. The tolerance to re-irradiation of heavily irradiated human skin. *British Journal of Radiology*. 50, 573.

CHAPTER 7

LAMERTON, L.F. and LORD, B.I., 1964. Studies of cell proliferation under continuous irradiation. *National Cancer Institute Monograph No. 14*. pp 185-198.

MASUDA, K., WITHERS, H.R., MASON, K.A. and CHEN, K.Y., 1977. Single dose-response curves of murine gastrointestinal crypt stem cells. *Radiation Research*. 69, 65.

HENDRY, J.H., ROSENBERG, I., GREENE, D. and STEWART, J.G., 1976. Tolerance of rodent tails to necrosis after daily fractionated X-rays or D-T neutrons. *British Journal of Radiology*. 49, 690.

APPENDIX II

WITHERS, H.R., BRENNAN, J.T. and ELKIND, M.M., 1970. The response of stem cells of intestinal mucosa to irradiation with 14 MeV neutrons. *British Journal of Radiology*. 43, 796.

HENDRY, J.H. and POTTER, C.S., 1974. Cryptogenic cells and proliferative cells in intestinal epithelium. *International Journal of Radiation Biology*. 25, 583.

SIGDESTAD, C.P., SCOTT, R.M., HAGEMANN, R.F. and DARDEN, E.B., 1974. Intestinal crypt survival: The effects of cobalt-60, 250 kVcp X-rays and fission neutrons. *Radiation Research*. 52, 168.

LESHER, S. and BAUMAN, J., 1969. Cell kinetic studies of the intestinal epithelium: Maintenance of the intestinal epithelium in normal and irradiated animals. In *Human Tumor Cell Kinetics*. National Cancer Institute Monograph 30, Washington, DC. pp 185-198.

LESHER, J. and LESHER, S., 1974. Effects of single dose partial body X-irradiation on cell proliferation in the mouse small intestinal epithelium. *Radiation Research*. 57, 148.

HAMILTON, E., 1977. Differences in survival of mouse colon crypts after whole or partial-body irradiation. International Journal of Radiation Biology. 31, 341.